REPORT SERIES IN AEROSOL SCIENCE
N:o 233 (2020)

MASS SPECTROMETRY STUDIES ON VAPOURS FORMING ATMOSPHERIC AEROSOL PARTICLES

OLGA GARMASH

Institute for Atmospheric and Earth System Research
Faculty of Science
University of Helsinki
Helsinki, Finland

Academic dissertation

To be presented, with the permission of the Faculty of Science of the University of Helsinki, for public criticism in Athena auditorium 302, Siltavuorenpenger 3 A, on December 15th, 2020, at 14 o'clock.

Helsinki 2020

Author's Address: Institute for Atmospheric and Earth System Research
P.O. Box 64
FI-00014 University of Helsinki
olga.garmash@helsinki.fi

Supervisors: Associate Professor Mikael Ehn, Ph.D.
Institute for Atmospheric and Earth System Research
University of Helsinki

Assistant Professor Matti P. Rissanen, Ph.D.
Aerosol Physics Laboratory
University of Tampere

Reviewers: Associate Professor Nønne L. Prisle, Doc. Ph.D.
Nano and Molecular Systems Research Unit
University of Oulu

Research Professor Markus Olin, Ph.D.
Department of Nuclear Energy
VTT Technical Research Centre of Finland Ltd

Opponent: Professor Jacqueline Hamilton, Ph.D.
Department of Chemistry
University of York

ISBN 978-952-7276-47-1 (printed version)
ISSN 0784-3496
Helsinki 2020
Unigrafia Oy

ISBN 978-952-7276-48-8 (pdf version)
https://www.faar.fi/
Helsinki 2020

Acknowledgements

I conducted the research for this dissertation at the Division of Atmospheric Sciences at the Department of Physics and later on at the Institute for Atmospheric and Earth System Research (INAR). I would like to thank the heads of the Department for providing me with the research facilities. I would also like to thank Academician Professor Markku Kulmala for an opportunity to be a part of an inspiring and ever-challenging research community.

I thank Associate Professor Nønne Prisle and Research Professor Markus Olin for reviewing this thesis. I am grateful to Professor Jacqueline Hamilton for being my opponent.

I thank my supervisor Associate Professor Mikael Ehn for his time and wisdom, for his trust in me finding my own path in science, for support in no matter what I got myself into. I also thank my second supervisor, Assistant Professor Matti Rissanen for discussing everything in the world with me.

I thank all my co-authors and colleagues for all the discussions and help over the years. You have aided me a great deal in becoming the scientist that I am.

I am truly grateful to all current and former technical staff at INAR. Pekka, Petri, Frans, Pasi, Jarkko, Hannu and Eki – you have helped me so much on my experimental path. Not only I learned a great deal from you, but you also made me feel as a part of the team. I am also grateful to everyone working in Hyytiälä.

I want to thank people, who are my friends, partners in crime as well as colleagues on an occasion or two – Otso, Liine, Sara, Lisa, Fede, Diego, Katja, Rima, Jenni, Stephany, Anna, Lubna, Lauriane, Yanjun and others. I could not do it without you.

I want to thank my mom for raising me to be anyone I want, for support and trust. I am grateful to my family and friends. Lastly, I want to thank Matti for love and for being so very supportive and understanding of my passion for knowledge and science.

Olga Garmash
University of Helsinki, 2020

Abstract

Aerosol particles present in the atmosphere can affect climate, visibility and human health. Low-volatility vapours form a large fraction of aerosol particles through gas-to-particle conversion. Our knowledge of chemical composition of low-volatility vapours has greatly improved in recent years with the development of more sensitive analytical tools. It is now widely accepted that in addition to sulphuric acid (SA), bases (e.g., ammonia and amines) and ions, which have been identified already a decade ago, highly oxygenated organic molecules (HOM) are crucial for the first steps of particle formation and growth. The main goal of this thesis was to identify which organic and inorganic vapours contribute to atmospheric particle formation in different environments.

In this thesis, I aimed to 1) determine the role of HOM and SA in forming clusters and particles in the boreal forest; 2) identify the aerosol precursor vapours in a megacity; and 3) determine HOM composition and yield in laboratory oxidation of selected compounds emitted from these two environments. The primary tool that I used for investigating the vapours and clusters was an atmospheric pressure interface time-of-flight mass spectrometer (APi-TOF). It was applied to detect either natural ions or, when equipped with a nitrate chemical ionisation, electrically neutral vapours. To achieve the aims of the thesis, we conducted measurements at a boreal forest station in Finland and in Shanghai, China. In addition, we performed laboratory experiments in a flow reactor and an atmospheric simulation chamber.

In the boreal forest, we observed that neutral HOM and SA concentrations influenced the composition of natural negatively charged clusters. Specifically, the ratio between HOM and SA controlled which chemical pathway initiated charged particle formation at this site. In contrast, by comparing our Shanghai observations to laboratory studies, we could conclude that SA-dimethylamine clustering initiated the formation of particles and their initial growth. In the laboratory experiments, we studied HOM formation in oxidation of sesquiterpenes and aromatics, which are emitted from the boreal forest and human activity, respectively. Both experiments showed that HOM formed at high yields. In aromatic oxidation, multi-step oxidation reactions were very important in HOM formation.

The results of this thesis increased our understanding of vapours that participate in secondary aerosol formation in the atmosphere. Finally, the results underlined the utmost importance of combining ambient investigations with laboratory experiments in atmospheric science.

Keywords: aerosol particles, low-volatility vapours, highly oxygenated organic molecules

Contents

1 Introduction **9**

2 Background and theory **13**

2.1 Production and loss of vapours 13

2.1.1 Sulphuric acid 15

2.1.2 Highly Oxygenated Organic Molecules 16

2.2 Clustering 19

2.3 Growth of particles by vapour condensation 20

3 Methods **22**

3.1 Instrumentation 22

3.1.1 APi-TOF 22

3.1.2 CI-APi-TOF 25

3.1.3 Other Instrumentation 30

3.2 Atmospheric studies 31

3.3 Laboratory studies 32

4 Results and discussion **34**

4.1 Aerosol precursors in boreal forest 34

4.1.1 The role of HOM and SA in naturally charged ions 34

4.1.2 Factors driving ion-induced particle formation 37

4.2 NPF precursors in an urban atmosphere 39

4.3 Production of HOM in VOC oxidation 42

4.3.1 Anthropogenic VOC: aromatic 42

4.3.2 Biogenic VOC: a sequiterpene 45

5 Review of papers and the author's contribution **47**

6 Conclusions and outlook **48**

References **51**

List of publications

This thesis consists of an introductory review, followed by five research articles. In the introductory part, these papers are cited according to their roman numerals.

I Bianchi, F., **Garmash, O.**, He, X., Yan, C., Iyer, S., Rosendahl, I., Xu, Z., Rissanen, M. P., Riva, M., Taipale, R., Sarnela, N., Petäjä, T., Worsnop, D. R., Kulmala, M., Ehn, M., and Junninen, H. (2017). The role of highly oxygenated molecules (HOMs) in determining the composition of ambient ions in the boreal forest, *Atmos. Chem. Phys.*, 17: 13819-13831.

II Yan, C., Dada, L., Rose, C., Jokinen, T., Nie, W., Schobesberger, S., Junninen, H., Lehtipalo, K., Sarnela, N., Makkonen, U., **Garmash, O.**, Wang, Y., Zha, Q., Paasonen, P., Bianchi, F., Sipilä, M., Ehn, M., Petäjä, T., Kerminen, V.-M., Worsnop, D. R., and Kulmala, M. (2018). The role of H_2SO_4-NH_3 anion clusters in ion-induced aerosol nucleation mechanisms in the boreal forest, *Atmos. Chem. Phys.*, 18: 13231-13243.

III Yao, L.*, **Garmash, O.***, Bianchi, F., Zheng, J., Yan, C., Kontkanen, J., Junninen, H., Mazon, S.B., Ehn, M., Paasonen, P., Sipilä, M., Wang, M., Wang, X., Xiao, S., Chen, H., Lu, Y., Zhang, B., Wang, D., Fu, Q., Geng, F., Li, L., Wang, H., Qiao, L., Yang, X., Chen, J., Kerminen, V.-M., Petäjä, T., Worsnop, D.R., Kulmala, M. and Wang, L. (2018). Atmospheric new particle formation from sulfuric acid and amines in a Chinese megacity, *Science*, 361, 6399, 278-281. ***Authors with equal contribution.**

IV **Garmash, O.**, Rissanen, M. P., Pullinen, I., Schmitt, S., Kausiala, O., Tillmann, R., Zhao, D., Percival, C., Bannan, T. J., Priestley, M., Hallquist, Å. M., Kleist, E., Kiendler-Scharr, A., Hallquist, M., Berndt, T., McFiggans, G., Wildt, J., Mentel, T. F., and Ehn, M. (2020). Multi-generation OH oxidation as a source for highly oxygenated organic molecules from aromatics, *Atmos. Chem. Phys.*, 20: 515-537.

V Jokinen T., Kausiala O., **Garmash O.**, Peräkylä O., Junninen H., Schobesberger S., Yan C., Sipilä M. and Rissanen M.P. (2016). Production of highly oxidized organic compounds from ozonolysis of β-caryophyllene: laboratory and field measurements, *Boreal Env. Res.*, 21: 262-273.

List of abbreviations

APi-TOF	atmospheric pressure interface time-of-flight mass spectrometer
BCP	β-caryophyllene
CCN	cloud condensation nuclei
CI	chemical ionsation
CLOUD	the Cosmics Leaving Outdoor Droplets experiment
cps	counts per second
CS	condensation sink
DMA	dimethylamine
HOM	highly oxygenated organic molecules
IIC	ion-induced clustering
JPAC	Jülich Plant Atmosphere Chamber
LOD	limit of detection
m/z	mass-to-charge ratio
NPF	new particle formation
ppb	parts per billion, 10^{-9}
ppt	parts per trillion, 10^{-12}
ppq	parts per quadrillion, 10^{-15}
SA	sulphuric acid
SOA	secondary organic aerosol
VOC	volatile organic compounds
X	a vapour molecule

1 Introduction

The Earth's atmosphere consists of nitrogen, oxygen, argon, water vapour, carbon dioxide, and a myriad of other trace gases as well as aerosol particles. Aerosol particles are liquid or solid particles that are suspended in gas, for instance, in air. The term *aerosol* refers to a two-phase system containing both particles and the gas. Particle size ranges from about 1 nm to 100 μm in diameter, most of which are invisible at low concentrations (Hinds, 1999). In one cm^3 of air, there can be from a few particles in remote polar regions to over 1 000 000 particles in heavily polluted environments (Seinfeld & Pandis, 2016). While being small and often invisible, aerosol particles have a wide range of effects on climate and human health.

Aerosol particles have a direct and an indirect effect on climate (Lohmann & Feichter, 2005; IPCC, 2013; Fuzzi et al., 2015). By absorbing or scattering solar and terrestrial radiation, aerosol particles directly influence Earth's radiation balance. This process also reduces visibility. Such phenomena as *blue mountains* or *haze* are induced by the presence of aerosol particles and their interactions with visible light (Went, 1960; Tyndall, 1869). In addition, aerosol particles can act as cloud condensation nuclei (CCN) and thereby indirectly affect the climate by forming clouds and modifying their properties (Twomey, 1977, 1991; Albrecht, 1989). Cloud properties, in turn, also have a link to radiation balance and hydrological cycle (Holton, 2003). In estimating the radiative budget of the atmosphere and modelling the future climate, this indirect aerosol effect is associated with the largest uncertainty (IPCC, 2013). When both of the effects are summed, aerosol particles have a net negative impact on the radiation balance, i.e. a cooling effect.

Depending on the size and composition, aerosol particles can also have adverse health effects upon inhalation. Prolonged exposure to particulate pollution may cause cardiovascular and respiratory diseases (Dockery & Pope, 1994; Lelieveld et al., 2015). The smallest particles can enter the bloodstream and deposit in other organs, in addition to lungs (Kreyling et al., 2013). Furthermore, some aerosols may carry viruses and bacteria, making aerosols also relevant in disease transmission (Alsved et al., 2019).

Aerosol particles can be separated into primary and secondary (Holton, 2003). Primary particles are directly emitted to the atmosphere. Examples of their sources are mechanical processes, such as wave breaking and road dust re-suspension, or incomplete combustion, such as during biomass burning. In contrast, secondary particles form in

the air in gas-to-particle conversion. In this process, particles form by condensation of low-volatility vapours, i.e. compounds that have low saturation vapour pressure. These vapours are also known as *aerosol precursors*. In some favourable atmospheric conditions, the vapours can form stable molecular clusters that then grow in size by condensation. This phenomenon is known as New Particle Formation, NPF (Weber et al., 1996; Mäkelä et al., 1997). It has been estimated that a substantial fraction of the global CCN originates from secondary processes, including NPF (Merikanto et al., 2009; Gordon et al., 2017).

Typically, low-volatility vapours form in oxidation reactions of inorganic and organic compounds emitted from natural or anthropogenic (human activity) sources. Oxidation of sulphur dioxide (SO_2), emitted mainly from industry, forms one of the most important inorganic vapour in secondary aerosol formation - sulphuric acid (SA) (Holloway, 2010). SA is known for its ability to participate in NPF (Weber et al., 1996; Sihto et al., 2006; Kulmala et al., 2014). Another example of potential low-volatility vapours are organic vapours. They form in oxidation of volatile organic compounds (VOC), largest part of which are emitted from trees and vegetation (Guenther et al., 1995). Biogenic VOC are mainly terpenes (isoprene, monoterpenes and sesquiterpenes) and some oxygenated compounds, while anthropogenic VOC are different alkanes, small alkenes, alkynes and aromatics (Guenther, 2000; Baker et al., 2008). Low-volatility organic compounds can participate in NPF (Riipinen et al., 2012; Kirkby et al., 2016) and form secondary organic aerosol (SOA), which constitutes a substantial fraction of total organic aerosol in the atmosphere (Kroll & Seinfeld, 2008; Jimenez et al., 2009). In general, during oxidation in the atmosphere, only small fraction of the oxidised compounds will become low-volatile. The concentration of low-volatility vapours in the atmosphere is low in comparison to other trace gases, but they can be more effective in forming aerosol particles.

The detection and identification of aerosol precursor vapours is challenging and requires high-sensitivity analytical tools. Due to their low saturation vapour pressure, a large fraction of these molecules is lost in the sampling lines. In addition, the same property leads to very low atmospheric concentrations. For instance, daytime SA concentration varies approximately between 10^5 and $10^7\,\mathrm{cm}^{-3}$, which means that only every 4^{th} to 400^{th} molecule per quadrillion of air molecules is a sulphuric acid molecule (Mauldin III et al., 1999; Petäjä et al., 2009; Zhang et al., 2011). Therefore, instruments with low limits of detection and high sensitivity for low-volatility vapours are needed.

With the development of high-sensitivity mass spectrometers for ambient application, a new subgroup of organic vapours, highly oxygenated organic molecules (HOM), was identified (Ehn et al., 2012; Ehn et al., 2014). HOM were first discovered in the boreal forest air. With the help of laboratory tests, their formation was connected to oxidation of monoterpenes. HOM were hypothesized to be mainly low-volatile due to their high oxygen content and large molar mass (Ehn et al., 2014; Kurtén et al., 2016; Peräkylä et al., 2020). The discovery of HOM was very important, as HOM have a potential to close the gap in understanding of the growth of small particles as well as SOA formation in the atmosphere (Riipinen et al., 2011; Volkamer et al., 2007; Tröstl et al., 2016; Mohr et al., 2019).

The processes that form aerosol precursor vapours and secondary aerosol particles differ between environments: cities, fields, forests, coastal areas, remote marine areas, polar regions and other. Two environments that are studied in this thesis are a boreal forest and a city. The boreal forest represents about one third of all forested areas (Taggart & Cross, 2009) and is dominated by biogenic VOC emissions, primarily by monoterpenes, isoprene and sesquiterpenes (Tarvainen et al., 2007; Rinne et al., 2009). Cities, on the other hand, are heavily populated areas with large anthropogenic emissions and risks to human health from air pollution. The VOC that have the highest SOA potential among urban emissions are aromatics, which also contribute to the production of toxic tropospheric ozone (Hallquist et al., 2009). It is essential to study the formation of aerosol particles in both remote and urban environments, due to their potential implications on climate as well as on human health.

In this thesis, I identified and quantified various aerosol precursor vapours. Using high-resolution and high-sensitivity chemical ionisation mass spectrometry, we conducted ambient measurements as well as experiments in the laboratory. Figure 1 shows the schematic representation of the conducted studies. The main objectives of my thesis were:

1. to determine the roles of HOM and SA vapours in the formation of clusters and particles in the boreal forest (**Papers I** and **II**)
2. to identify aerosol precursor vapours in an urban environment (**Paper III**)
3. to determine HOM composition and yields in laboratory oxidation of important, but less studied from a HOM perspective, VOC: sesquiterpenes and aromatics (**Papers IV and V**).

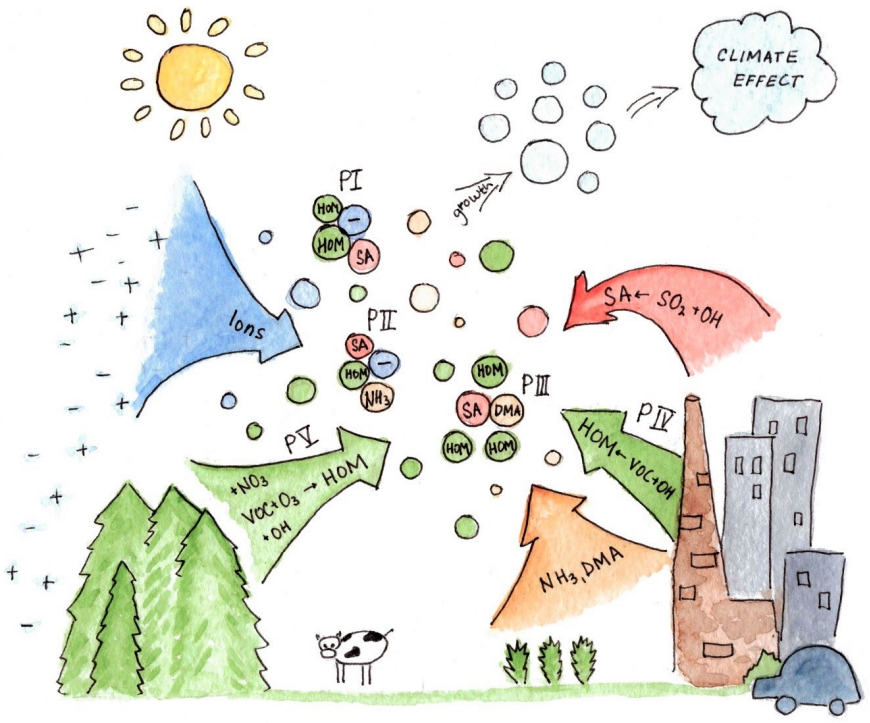

Figure 1: A schematic of atmospheric processes studied in this thesis. **Papers I**, **II** and **III** investigate aerosol precursor vapours in a forest and in a city. The vapours form clusters, which then can grow to larger particles by vapour condensation and become climate-relevant at larger sizes. **Papers IV** and **V** study the formation of HOM in oxidation of aromatic compounds and sesquiterpenes. VOC - volatile organic compounds; HOM - highly oxygenated organic molecules; SA - sulphuric acid; SO_2 - sulphur dioxide; NH_3 - ammonia; DMA - dimethylamine.

2 Background and theory

This section introduces the key concepts related to the formation of vapours, clusters and aerosol particles. Low-volatility vapours in the atmosphere form primarily through oxidation. They can either form molecular clusters or condense on pre-existing aerosol particles. The formation and consequent growth of particles to larger sizes makes aerosol particles relevant in the climate system.

2.1 Production and loss of vapours

Vapour is defined as a gas below its critical temperature (Lewis & Evans, 1997), which means that it can condense. Vapours are created by molecules escaping the liquid or solid phase in processes of evaporation and sublimation, respectively. In equilibrium conditions of vapour with the condensed phase, the amount of vapour molecules evaporating and condensing is equal, and a partial pressure exerted by the gas-phase molecules is called saturation vapour pressure (Atkins, 1998; Vehkamäki & Riipinen, 2012). The lower the saturation vapour pressure is, the lower is the required concentration for a vapour to condense, the lower is the *volatility* of a vapour. The amount of vapour in the air can be described by its partial vapour pressure, which, with an assumption of ideal gas, is proportional to vapour concentration. Concentration, a quantity that is typically measured, can help us to assess the vapour's ability to condense and form aerosol particles. The change in the molecular concentration of vapour X in time (typically is defined per second) depends on the balance of source and sink rates:

$$\frac{d[X]}{dt} = \text{Source}_X - \text{Sink}_X \tag{1}$$

In addition to physical processes, vapours are produced in the atmosphere via chemical reactions. For low-volatility vapours needed for secondary aerosol formation, oxidation is the most important chemical source. Oxidation is typically initiated by one of the most common oxidants (electron acceptors, (Atkinson & Aschmann, 1989)), such as hydroxyl radical (OH), ozone (O_3) and nitrate radical (NO_3), or in some cases by other oxidants, such as chlorine atoms or stabilized Criegee Intermediates (Seinfeld & Pandis, 2016; Thornton et al., 2010; Mauldin III et al., 2012). The oxidants attack compounds

in the atmosphere creating radicals, molecules with an unpaired electron. Radicals can react with molecular oxygen (O_2) becoming more oxygenated and less volatile.

An important parameter controlling the vapour production in oxidation reactions is a molar yield. In chemical kinetics, a molar yield is a branching ratio of a certain reaction leading to the formation of a molecule X. However, if intermediates of the reactions are unknown, the yield of vapours may be defined as the amount of produced vapour in relation to the reacted amount of original precursor (**Paper IV**). Similar definition is commonly used in quantifying the potential of VOC to form SOA, where a yield is the SOA mass produced in relation to the amount of consumed VOC (Kroll & Seinfeld, 2008).

A sink for vapours can also be a chemical reaction, but also dry and wet deposition. One of the main losses of low-volatility vapours in the atmosphere is their condensation onto the surface of the aerosol particles. Such loss rate is described by the *condensation sink* term (CS) (Kulmala et al., 2001). CS is calculated knowing aerosol number size distribution and properties of the vapour molecules as follows:

$$\mathrm{CS} = 2\pi D \sum_{d_p} \beta_{m,d_p} d_p N_{d_p}, \tag{2}$$

where β_{m,d_p} is the correction factor for the transition regime (particles are only slightly larger than air molecules) (Kulmala et al., 2012), d_p is the mean diameter of particle size bins, and N_{d_p} is the concentration of particles in each size bin $\mathrm{d_p}$. D is the diffusion coefficient of a specific molecule in air, which can be estimated based on the empirical equation provided by Fuller et al. (1966). Estimating D requires the molar mass and the atomic composition for a condensing molecule. CS is an upper (collision) limit of loss estimation for most of the atmospheric vapours (see section 2.3). If the loss rate is calculated using CS, it assumes irreversible condensation on particle surface.

Low-volatility vapours are critical in the formation of secondary aerosol particles. Sections 2.1.1 and 2.1.2 review the formation of sulphuric acid and HOM, respectively, which are the primary vapours studied in this thesis.

2.1.1 Sulphuric acid

Sulfuric acid (SA, H_2SO_4) predominantly forms in the gas-phase in oxidation of sulfur dioxide (SO_2) with OH (Seinfeld & Pandis, 2016). In presence of a third molecule (M), this reaction produces $HOSO_2^{\bullet}$ radical. $HOSO_2^{\bullet}$ will react with a molecular oxygen and form hydroperoxy radical ($HO_2^{\bullet}$) and sulphur trioxide (SO_3), which in presence of water vapour will form sulphuric acid as shown below:

$$SO_2 + OH + M \longrightarrow HOSO_2^{\bullet} + M$$
$$HOSO_2^{\bullet} + O_2 \longrightarrow HO_2^{\bullet} + SO_3$$
$$SO_3 + H_2O + M \longrightarrow H_2SO_4 + M$$

A major part of SO_2 is emitted due to anthropogenic activity; however, some is also emitted from volcanoes as well as forms in oxidation of algae-emitted dimethylsulfide (dimethylsulfide in addition to SO_2 can also form SA through methanesulfonic acid) (Holloway, 2010). As OH radicals are mainly produced photochemically, SA concentrations are highest during the day ranging from 10^5 to $10^8\,cm^{-3}$ for most environments (Mauldin III et al., 1999; Petäjä et al., 2009; Zhang et al., 2011). Night-time concentration of SA is typically much lower; however, in heavily polluted environments it can reach $10^6\,cm^{-3}$ due to night-time oxidation processes (**Paper III,** Guo et al., 2020b).

In many locations around the world, a positive relationship between the particle formation rate and SA concentration during NPF events has been established (Kuang et al., 2008). This led to a hypothesis that SA is the most important precursor for new aerosol particles. While it has been confirmed that SA can in fact form molecular clusters, the typical ambient concentrations are too low to account alone for particle formation rates (Kirkby et al., 2011) or the particle growth by condensation during NPF events in the boundary layer (Boy et al., 2005; Riipinen et al., 2011). With the decreasing trend of anthropogenic SO_2 emissions, clarifying the role of SA in clustering and particle growth is important so that the future impact of aerosol particles on climate can be estimated (Makkonen et al., 2012).

2.1.2 Highly Oxygenated Organic Molecules

Highly oxygenated organic molecules (HOM) are another group of low-volatility compounds that is now known to contribute at early stages of particle formation. Ehn et al. (2010) first observed these high molecular mass molecules in natural ions at SMEAR II station located in the Finnish boreal forest (see section 3.2). The authors hypothesised these molecules to be organic. Later study that combined field measurements with laboratory experiments confirmed that these compounds were highly oxygenated products of monoterpene oxidation with night-time composition of HOM being almost identical to α-pinene ozonolysis (Ehn et al., 2012). These HOM were C_5-C_{20} molecules mainly clustered with NO_3^- ions. Following this natural clustering mechanism, nitrate chemical ionisation was applied to detect also electrically neutral HOM (Ehn et al., 2014). Due to high oxygen content and mass of HOM, they were at first considered to be extremely low-volatility vapours (Ehn et al., 2014). However, later on it became clear that HOM can also be semi- and low-volatile (Kurtén et al., 2016; Tröstl et al., 2016; Peräkylä et al., 2020). Nevertheless, HOM have a potential to explain some of the observed growth of aerosol particles during NPF events, for instance in the boreal forest (Ehn et al., 2014; Mohr et al., 2019).

A recent review of HOM studies by Bianchi et al. (2019) suggested a set of HOM definitions. A molecule could be defined as a HOM if:

1. it is a molecule formed in autoxidation of peroxy radicals (RO_2).
2. it has formed in the gas-phase and at atmospheric conditions.
3. it has six or more oxygen atoms.

HOM can be monomers, which form from a single VOC molecule. In addition, HOM can be dimers, which contain two covalently bonded products of VOC oxidation (Bianchi et al., 2019). HOM formation pathway is described below in more detail.

For VOC to form HOM, it has to undergo a series of reactions. At first, VOC reacts with an oxidant in the gas-phase, and almost always forms an initial RO_2 radical. Then, the oxidation propagates via autoxidation. *Autoxidation* is a series of subsequent intra-molecular H-shifts and O_2 additions (Crounse et al., 2012; Crounse et al., 2013). The process is schematically shown in Figure 2. Specifically, a peroxy group of

RO_2 radical (I on Figure 2) abstracts a hydrogen atom from a carbon atom within the same molecule which results in an alkyl radical with a hydroperoxide functionality (II on Figure 2). An oxygen molecule (O_2) can then attach to an unpaired electron and create yet another RO_2 radical (III on Figure 2). If this process leads to the formation of molecules with six or more oxygen atoms, HOM (radical) is formed.

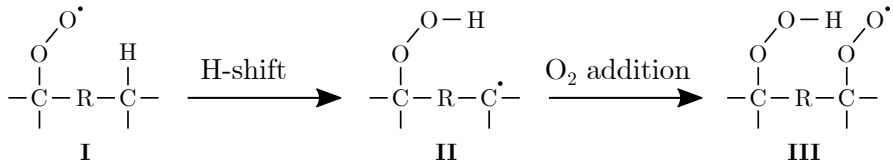

Figure 2: Schematic showing an example molecule undergoing autoxidation. R denotes a hydrocarbon chain. Figure is based on Ehn et al. (2014).

H-shift toward peroxyl can happen from different carbon atoms. The rate of H-shift is dependent on the position of peroxy group in relation to the favourable H-donor carbon (Orlando & Tyndall, 2012; Vereecken & Francisco, 2012; Rissanen et al., 2015; Kurtén et al., 2015). In addition, the H-shift is affected by substitutions on the carbon atom as well as temperature (Bianchi et al., 2019). The rate of H-shifts as well as the concentration of RO_2 and other species in the system will determine the probability of autoxidation happening as it proceeds in competition with other unimolecular and bimolecular reactions.

Unimolecular and bimolecular reactions can propagate and terminate the oxidation chain. Propagating reactions create new radicals, while terminating reactions convert a radical into a closed-shell molecule, i.e. all electrons are paired. Most of HOM in the atmosphere are measured as close-shell molecules, as the lifetime of radicals is short (Ehn et al., 2012, **Paper I**). An example of unimolecular termination is the ejection of OH group, while an example of bimolecular termination is a reaction of RO_2 with another RO_2, HO_2 or NO. Most of termination reactions result in monomer products; however, cross reaction of two RO_2 radicals may also form covalently bonded dimers sometimes. Chains of propagating and terminating reactions create highly functionalised compounds with reduced volatility unless fragmentation takes place. These pathways are described in detail in **Papers IV and V** and in other literature

(Finlayson-Pitts & Pitts, 2000; Vereecken & Francisco, 2012; Orlando & Tyndall, 2012; Rissanen et al., 2014; Rissanen et al., 2015; Bianchi et al., 2019; Peräkylä, 2020).

After HOM discovery, a number of studies confirmed the importance of autoxidation and HOM formation in several different VOC systems. Most of the tested biogenic terpenoids, such as isoprene, α-pinene, β-pinene, limonene, and myrcene and some sesquiterpenes, formed HOM in reaction with O_3 (Ehn et al., 2014; Jokinen et al., 2015; Richters et al., 2016b, **Paper V**). In comparison with ozonolysis, oxidation of terpenoids with OH radicals in some cases produced more HOM (isoprene, β-pinene) and in some cases less (α-pinene, limonene) (Ehn et al., 2014; Jokinen et al., 2015). The molar yields of HOM differed among VOC, which could be attributed to the differences in their structures. In studying structure-dependence of HOM formation, cyclic alkenes, such as cyclohexene, were used as surrogates both experimentally and computationally (Rissanen et al., 2014; Rissanen et al., 2015; Mentel et al., 2015; Berndt et al., 2015; Berndt et al., 2016; Hyttinen et al., 2017). In addition, HOM were also detected in OH-initiated oxidation of aromatic VOC (Wang et al., 2017; Molteni et al., 2018, **Paper IV**). These laboratory single-component experiments provide basis for understanding of fundamental chemistry and complex atmospheric mixtures.

In addition to the boreal forest in Finland (Ehn et al., 2014; Yan et al., 2016, **Paper I**), HOM were also detected in other areas. For instance, HOM were detected in Germany by Jokinen et al. (2014) near agricultural pastures and forest as well as by Kürten et al. (2016a) at a rural site near diary farms. Krechmer et al. (2015), Lee et al. (2016) and Massoli et al. (2018) identified HOM at rural mixed forest in USA, where isoprene emissions dominate. In alpine environment, HOM were detected by Bianchi et al. (2016) and Frege et al. (2017). Some of the compounds detected by Li et al. (2020) in French pine-dominated forest could also be classified as HOM. Among urban environments, HOM were seen near an oil refinery (Sarnela et al., 2015), in cities of Shanghai, Beijing and Barcelona **Paper III**, Brean et al., 2019; Brean et al., 2020. In several field studies, HOM were connected to clustering and NPF (Kulmala et al., 2013; Jokinen et al., 2017; Rose et al., 2018; Bianchi et al., 2016) as well as were found in the particle phase (Mutzel et al., 2015; Lee et al., 2016; Mohr et al., 2019). The potential role of HOM in the atmosphere can be two-fold: contribution to NPF as well as SOA.

2.2 Clustering

Clusters are agglomerates of two or more molecules that form upon molecular collisions. Most molecules in air, such as N_2 and O_2 will not interact during a collision and will bounce off (Kupiainen-Määttä, 2016). However, some compounds will interact through intermolecular forces, e.g., Van der Waals forces (Israelachvili, 2011). Depending on the strength of the attracting force, clusters can linger in the atmosphere or they can evaporate back to their gas-phase constituents. Among clusters, the force is stronger with ion - neutral molecule and acid - base molecule interactions (Kupiainen-Määttä, 2016).

Electrically charged clusters are examples of stable clusters that are almost always present in the atmosphere (Manninen et al., 2009b). They are created by ionized molecules colliding with neutral molecules and constitute so-called cluster ions. The cluster ions are typically below 1.6 nm in diameter (Hõrrak et al., 2000; Hirsikko et al., 2005). For instance, $H_2SO_4 \cdot HSO_4^-$, $HNO_3 \cdot HSO_4^-$ and $HNO_3 \cdot NO_3^-$ are examples of negatively charged cluster ions (Ehn et al., 2010). The ion - neutral molecule clustering mechanism is also the basic principle for chemical ionisation mass spectrometry. In addition to charged clusters, electrically neutral clusters are also present in the atmosphere, though their detection, especially in sizes below 1.6 nm, is challenging (Kulmala et al., 2012; Kontkanen et al., 2017).

Clustering is the first step in new particle formation (Kulmala et al., 2013). NPF is initiated when a stable cluster grows in size by an attachment of other molecules or clusters. In some chemical systems, there is an energy barrier that a cluster has to overcome to become more likely to grow than to evaporate, a process known as *nucleation* (Vehkamäki, 2006). However, in other systems, the cluster growth may be only kinetically limited by the rate of molecular collisions (Vehkamäki & Riipinen, 2012). Sulphuric acid can form stable clusters in presence of water, bases, such as ammonia (NH_3) and dimethylamine (DMA), and organics (for instance, HOM) (Coffman & Hegg, 1995; Ball et al., 1999; Kurtén et al., 2008; Kirkby et al., 2011; Almeida et al., 2013; Riccobono et al., 2014). SA forms very stable clusters with its conjugate base, bisulphate (HSO_4^-). As a result, ions can enhance the cluster stability and increase particle formation rates in NPF that involves SA when clustering is not collision-limited, as was found for ternary SA-DMA-H_2O system (Almeida et al., 2013). Ions can also enhance the stability of pure HOM clusters, which recently were shown to initiate

NPF in laboratory simulations (Kirkby et al., 2016). The ion enhancement in cluster stability is most pronounced at lower concentrations of precursor vapours in systems involving SA, NH_3 and HOM.

Cluster population is affected by various physical and chemical processes. For instance, lower temperature enhances cluster stability as vapours become lower in volatility (Kirkby et al., 2011; Kürten et al., 2016b). Clusters can be lost by growth to larger sizes provided low-volatility vapours are readily available. They can also be scavenged in coagulation with pre-existing aerosol particles (Hirsikko et al., 2011). The composition of trace gases in the air will also influence the cluster chemistry. For instance, ion cluster composition may be driven by the concentration of certain acidic or basic vapours (Eisele, 1989a, 1989b; Ehn et al., 2010, **Papers I and II**). Similarly to vapours (section 2.1), at a given atmospheric conditions, the cluster concentration will depend on the sources and sinks, and, therefore, mainly on the availability of low-volatility vapours and background aerosol particle concentration.

2.3 Growth of particles by vapour condensation

Condensation is a process of a phase transition from gas to liquid. The phase change happens if the actual vapour pressure exerted by vapour molecules is greater than the saturation vapour pressure of that liquid. In that instance, the vapour is called *supersaturated* (Vehkamäki & Riipinen, 2012). The ratio of partial pressure of a vapour and its saturation vapour pressure defines *saturation ratio* (S) and can indicate if a compound is preferentially condensing (S>1), evaporating (S<1) or existing in an equilibrium (S=1) with liquid phase. The above definitions are usually applied to one-component system where the liquid surface is flat. In multi-component system, the saturation vapour pressure of a compound will be scaled by its molar fraction in the condensed phase. This scaled parameter is termed *equilibrium vapour pressure* and is the main principle of Rault's law (Vehkamäki & Riipinen, 2012; Seinfeld & Pandis, 2016). The interactions between vapour and solid can be described analogously to vapour-liquid system (Vehkamäki & Riipinen, 2012).

Condensation of vapours is the main process in which small particles can grow to larger sizes. However, the condensation proceeds in competition with evaporation (Yli-Juuti et al., 2020). Due to high surface curvature of small particles, it is easier for vapour molecules to evaporate from them. In comparison to flat liquid surface,

molecules at the curved particle surface have a reduced amount of interactions with neighbouring molecules. This phenomenon is known as Kelvin effect, which states that the equilibrium vapour pressure over a curved surface is greater than over a flat surface of the same compound (Thomson, 1871; Seinfeld & Pandis, 2016). Therefore, the smaller the particle diameter is, the larger is the curvature, the more vapour is needed for condensation. Alternatively, the vapour of lower volatility is needed.

Volatility is another way of referring to the saturation vapour pressure of a compound. The lower the saturation vapour pressure of a compound, the lower is its volatility. Low-volatility vapours are needed to grow small particles at atmospheric conditions (Kulmala et al., 1998; Riipinen et al., 2011). When talking about organic vapours, one of the useful frameworks is the two-dimensional volatility basis set (VBS) (Donahue et al., 2011). The VBS separates organic vapours by their oxygen-to-carbon ratio and their saturation concentration C^*, which is proportional to saturation vapour pressure. Based on C^*, the organics are divided into volatile, intermediate-, semi-, low- and extremely low- volatile compounds (VOC, IVOC, SVOC, LVOC, and ELVOC respectively). HOM can be mainly classified into ELVOC, LVOC and SVOC (Tröstl et al., 2016; Bianchi et al., 2019; Yan et al., 2020). ELVOC will be most important for condensing on smallest particles. As particles grow in size, LVOC and SVOC will start to contribute to particle growth (Tröstl et al., 2016). As particles grow in size, Kelvin effect becomes less important and partitioning of vapours to the condensed phase is driven by total organic aerosol mass. At low aerosol concentrations, only vapours with lowest volatility will partition, while at higher concentrations of organic aerosol, also semi-volatile species will partition to the condensed phase (Seinfeld & Pandis, 2016).

As particles reach sizes of CCN, they can be activated into cloud droplets by water condensation. This activation process is described by Köhler theory that takes into account both Rault and Kelvin effects (Köhler, 1936; Seinfeld & Pandis, 2016). The exact diameter of activated CCN particles will depend on their composition and on the degree of supersaturation of water vapour (Kerminen et al., 2012; Prisle et al., 2010). As particles become larger in size or form cloud droplets, they become relevant for the climate.

3 Methods

In this section, I present the main experimental tools used in this thesis. In addition, I introduce the atmospheric field sites and the set-ups of laboratory experiments.

3.1 Instrumentation

The development of an atmospheric pressure interface time-of-flight mass spectrometer (APi-TOF) allowed for studying clusters and low-volatility vapours with a high level of detail (Junninen et al., 2010; Ehn et al., 2010). Used as it is, APi-TOF can provide the molecular information of naturally charged ions and ion clusters, as was done in **Papers I, II, III and V**. In addition, coupled with NO_3^- chemical ionization inlet (CI), it can detect neutral HOM, sulphuric acid and other vapours (used in all **Papers I-V**) (Jokinen et al., 2012; Ehn et al., 2014). This and other instruments used in this thesis are described in more detail below.

3.1.1 APi-TOF

APi-TOF is schematically presented in Figure 3. The main part of the instrument consists of an atmospheric pressure interface (APi) coupled to a time-of-flight (TOF) mass spectrometer (Junninen et al., 2010). In addition, a sampling inlet is constructed to minimise the diffusional losses of ambient ions. The sampling is conducted with shortest possible straight stainless steel tube. The outer sampling line is actively pumped with an approximate 8 to 10 lpm. From the centre of that tube, a smaller flow (about 5 lpm) is directed as close as possible to the critical orifice. The two sampling flows are maintained to have similar velocity and to be laminar. The flow which guides the ions into the APi-TOF mass spectrometer through critical orifice is about 0.8 lpm.

APi-TOF consists of few differentially pumped sections. APi consists of two quadrupoles (Q1 and Q2 on Figure 3) and an ion lens assembly that guide and focus the ions while gradually pumping out the air and reducing the pressure. This interface allows sampling directly from ambient pressure through a 0.3 mm critical orifice. After APi, sample ions enter a TOF mass spectrometer, with pressure of about 10^{-6} mbar. In TOF, the ions are pulsed to follow a V-shaped flight path. At the end

of the flight path they hit the detector, a micro-channel plate. The time of the arrival and the strength of the signal are recorded.

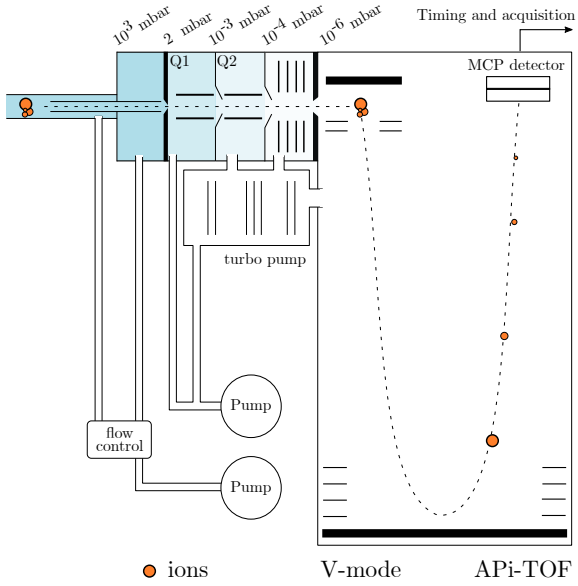

Figure 3: The schematic of an APi-TOF mass spectrometer. Q1 and Q2 denote quadrupoles. The critical orifice is located before Q1. MCP denotes a micro-channel plate. The size of the ions is proportional to their m/z. Figure is based on Junninen (2013).

Smaller ions arrive first, while larger ions arrive last. The time-of-flight is then converted to mass-to-charge ratio (m/z). Ions from approximately 50 to 2000 m/z can be detected. The averaged spectrum is typically saved with 1 to 10 second time resolution to allow for reasonable signal-to-noise ratio. APi-TOF can detect ions of one polarity at a time. In this thesis, only negative polarity was utilized, because clustering with bisulphate (HSO_4^-) and nitrate (NO_3^-) anions was investigated.

To be able to identify the atomic composition of ions, a careful calibration of time-of-flight to mass-to-charge ratio is performed using known ions. An example set of such ions used in **Paper I** is presented in Table 1. The set of peaks used for calibration is not universal and should be adjusted based on measurement location and time of the day.

The calibration ions should have high signal-to-noise, be located at a representative m/z range and should be single peaks, i.e. the only ion present at a particular m/z. Due to low ion concentrations in the ambient air, it is common to average the mass spectrum over one to three hours for reliable peak identification. The signal obtained from APi-TOF was processed using tofTools package for MATLAB following the steps described by Junninen (2013).

Table 1: Ions that were used in **Paper I** for calibration of mass-to-charge axis (Ehn et al., 2010; Ehn et al., 2012; Yan et al., 2016). It is also indicated if ions are mainly found during the day or night.

Exact mass	**Composition**	**Time**	**Note**
96.9601	HSO_4^-	day	bisulphate, deprotonated SA
103.0037	$C_3H_3O_4^-$	day/night	deprotonated malonic acid
124.9840	$HNO_3 \cdot NO_3^-$	night	nitric acid-nitrate cluster
159.9557	$HNO_3 \cdot HSO_4^-$	day	nitric acid-bisulphate cluster
165.9993	$C_3H_4O_4 \cdot NO_3^-$	day/night	malonic acid-nitrate cluster
194.9275	$H_2SO_4 \cdot HSO_4^-$	day	SA-bisulphate cluster
292.8949	$(H_2SO_4)_2 \cdot HSO_4^-$	day	SA-bisulphate cluster
308.0623	$C_{10}H_{14}O_7 \cdot NO_3^-$	day/night	HOM
340.0521	$C_{10}H_{14}O_9 \cdot NO_3^-$	day/night	HOM
355.0630	$C_{10}H_{15}O_9N \cdot NO_3^-$	day	HOM
372.0420	$C_{10}H_{14}O_{11} \cdot NO_3^-$	day/night	HOM
555.1679	$C_{20}H_{31}O_{13}N \cdot NO_3^-$	night	HOM
556.1519	$C_{20}H_{30}O_{14} \cdot NO_3^-$	night	HOM

As seen in Table 1, in addition to single molecular ions, API-TOF can also detect molecular clusters. Examples are bisulphate and nitrate clusters with molecules of sulphuric acid and organics, clusters with sulphuric acid and bases, such as ammonia and amines. Lists of identified ions in APi-TOF can be found in literature for laboratory experiments (Ehn et al., 2012; Schobesberger et al., 2013; Riccobono et al., 2014; Bianchi et al., 2014; Frege et al., 2018) and for the atmosphere (Junninen et al., 2010; Ehn et al., 2010; Ehn et al., 2012; Bianchi et al., 2016; Frege et al., 2017, **Paper V**).

APi-TOF is a powerful tool for detecting natural clusters in the atmosphere, as there is no pre-treatment of the sample. However, low pressure and electric field inside of the

instrument can lead to cluster fragmentation (Passananti et al., 2019). In addition to de-clustering, some portion of ions will be lost due to diffusion in the sampling line as well as inside of the TOF chamber. The total ion signal will be, therefore, from about 5 to 30 counts per second (cps) in typical atmospheric boundary layer measurement. As a result it is challenging to invert the real ambient ion concentration. If transmission of the instrument is known, the concentration of ion X can be calculated as follows:

$$[X] = \frac{\text{signal}_X}{t \times f}, \tag{3}$$

where signal for an ion X is in counts per second, t is the correction factor for transmission, including losses, and f is the flow through the critical orifice. Using modelling, as suggested by Passananti et al. (2019), it is also possible to estimate ion cluster concentrations, but more commonly transmission calibration against an electrometer has been applied (Junninen et al., 2010).

3.1.2 CI-APi-TOF

In comparison to ions, much more molecules in the atmosphere are present in the electrically neutral state. To allow for their detection in a mass spectrometer, they need to be charged (ionised). One of the most suited ionisation methods for atmospheric vapours and clusters is chemical ionisation (CI). CI allows for soft ionisation minimizing fragmentation during the process. APi-TOF with a CI inlet in front of it comprises CI-APi-TOF mass spectrometer (Jokinen et al., 2012). Ionisation by nitrate ion (NO_3^-) has been used for detection of sulphuric acid and its clusters (Eisele & Tanner, 1993). Recently, following discovery of HOM as clusters with NO_3^- in ions, this ionisation method has been applied for detection of neutral oxygenated organics, including HOM (Ehn et al., 2014).

The schematic of a CI inlet is shown in Figure 4. The sample is taken from the ambient air through a straight stainless steel tube. A sheath flow carrying nitric acid (HNO_3) is guided coaxially around the sampling line. In the ion source region, X-ray or ^{241}Am source is used to ionise HNO_3 to NO_3^-. Ionisation source ionises nitric acid in the sheath flow and the formed ions will have composition of $(HNO_3)_n \cdot NO_3^-$ as neutral nitric acid and nitrate ion bind strongly to each other (Hyttinen et al., 2015). Sheath flow is dry

particle-free air, which is also filtered for SO_2 to minimize sulphuric acid background signal at peaks corresponding to HSO_4^- and $HNO_3 \cdot HSO_4^-$.

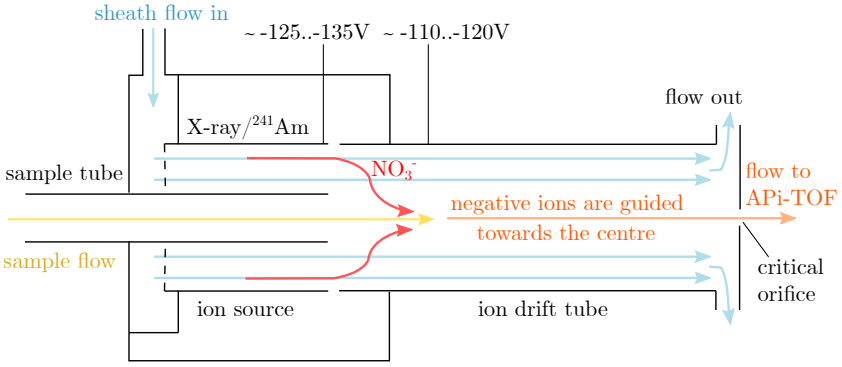

Figure 4: Schematic representation of chemical ionisation inlet. It is attached in front of the critical orifice to APi-TOF replacing the ambient ion inlet (Figure 3). Ion source and drift tube voltages are ballpark suggestions.

At a point where the sheath flow meets the sample flow, NO_3^- ions begin to move towards the centre of the sample flow guided by an electric field. At this point, the sample tube should be aligned with the end of the ion source as shown in Figure 4. Electric field is created by applying voltage to the ion source and the ion drift tube (typically 10-15 V difference). The ions interact with the sample molecules in the drift tube for about 200 ms depending on the chosen flows. The excess flow is pumped out from the inlet while the ions are directed through the critical orifice and into the APi-TOF.

The co-axial design of the CI inlet minimises the wall loss of the sampled molecules. Typical values for sheath flow and flow out (see Figure 4) is 20 and 30 lpm respectively, but higher flows can also be used. The flows should be laminar as turbulence will induce wall losses and dilution of the sample. A check for turbulence can be done by switching off the electric field in the inlet. Stable near-zero ion count during that test will confirm the absence of turbulence. The typical flow for HNO_3 into the sheath flow is from 5 to 10 mlpm.

Detection of molecules and clusters

Nitrate clusters ionise the sample molecules either via adduct formation or via proton transfer. Most of the detected vapours, including HOM, SA, and organic acids, are detected via adduct formation with NO_3^- (equation 4). In addition, some of the acids, such as sulphuric acid, methanesulfonic acid, iodic acid, and dicarboxylic acids, also undergo proton transfer reaction as shown in equation 5. In equations 4 and 5, X depicts a compound of interest that is being ionised.

$$X + (HNO_3)_n \cdot NO_3^- \rightarrow X \cdot NO_3^- + (HNO_3)_n \tag{4}$$

$$XH + (HNO_3)_n \cdot NO_3^- \rightarrow X^- + (HNO_3)_{n+1} \tag{5}$$

NO_3^- chemical ionisation is sensitive and selective to oxidised organics. Based on computational study by Hyttinen et al. (2015), a molecule should contain at least two hydrogen bond donor groups, such as hydroxy (OH-) or hydroperoxy (OOH-), to form detectable clusters with NO_3^-. The position of these groups on the molecule will also play a role during ionisation, though the ionisation efficiency can be well approximated based only on oxygen content (Hyttinen et al., 2018). In addition, compounds, such as nitrophenol, that contain one -OH and one -NO_2 group can also cluster with NO_3^- (Hyttinen et al., 2018). The selectivity of nitrate ions towards highly functionalised molecules and nearly "wall-less" set-up of the CI-inlet, which minimizes sampling losses, make this method suitable for detecting HOM, and especially HOM dimers rarely observed by other chemical ionisation techniques (Riva et al., 2019).

In addition to individual molecules, CI-APi-TOF can also detect ambient neutral clusters. Detection of clusters is tricky as upon collision with NO_3^- they can rearrange and break apart to take a more stable form. In SA-DMA-NH_3 experiments, clusters have been detected in a form of only SA-bisulphate, SA-DMA-bisulphate and SA-DMA-NH_3-bisulphate clusters (Bianchi et al., 2014). In this system, some ammonia and DMA will evaporate upon charging (Kürten et al., 2014; Ortega et al., 2014; Rondo et al., 2016). In addition, iodic clusters can be detected (Sipilä et al., 2016). No neutral SA-NH_3 or organic-containing clusters have been detected with nitrate CI-APi-TOF so far.

Identification of the peaks

Similarly to measurements with APi-TOF, the time-of-flight has to be converted to m/z using a set of known compounds in the mass spectrum. In nitrate chemical ionisation, $(HNO_3)_{0-2}{\cdot}NO_3^-$ clusters can be used for calibration. However, due to high concentrations of reagent ions, their peaks may be distorted. Therefore, the results may be better if the calibration is done on isotopes, for instance, $N^{18}OO_2^-$. In addition to reagent ions, larger molecules should also be included into calibration, for example, HOM compounds that are listed in Table 1.

Compounds detected with CI-APi-TOF have been identified in numerous field and laboratory studies. The identification of certain peaks uses exact mass of the peak as well as isotopic pattern. Nitrogen and hydrogen rules can be used for assigning the molecular composition for molecules of typical atmospheric relevance. Hydrogen rule determines the upper limit of hydrogen atoms in a molecule as 2C+N+2, where C and N are the number of carbon and nitrogen atoms respectively. Nitrogen rule states that if a molecule has an odd nominal mass, it will have an odd number of nitrogen atoms, which is reversed if a molecule is an ion or a radical (**Paper I**). The lists of identified compounds can be found in the literature, often in supplementary material (Ehn et al., 2014; Rissanen et al., 2014; Mentel et al., 2015; Berndt et al., 2015; Bianchi et al., 2016; Kürten et al., 2016a; Yan et al., 2016; Richters et al., 2016a; Frege et al., 2018; Molteni et al., 2018; Brean et al., 2019; McFiggans et al., 2019; Brean et al., 2020; Heinritzi et al., 2020; Fang et al., 2020; Wang et al., 2020, **Papers III-V**).

Determining the concentration

The calibration standards for most of the compounds of interest, such as HOM, are not available. Most common calibration of CI-APi-TOF is performed with sulfuric acid to determine the collision-limited calibration coefficient (Kürten et al., 2012). The same calibration coefficient has been applied to HOM. While it has become apparent using computational methods that not all the HOM are detected with the collision limit (Hyttinen et al., 2015), estimation of accurate detection efficiencies for all the observed HOM are not yet possible (Hyttinen et al., 2018). Therefore, the determined concentration of compounds from CI-APi-TOF typically represents a lower limit (provided the transmission has been accounted for) Ehn et al., 2014; Berndt et al., 2015, **Paper IV**.

The concentration for a given molecule can be calculated using calibration coefficient and normalised signal of ions corresponding to that molecule following an equation 6 (Jokinen et al., 2012):

$$[X] = C_f \times \frac{\sum_i X_i \cdot NO_3^-}{\sum_{i=0}^{2} (HNO_3)_i \cdot NO_3^-} \tag{6}$$

where C_f is the calibration coefficient and $[X]$ is the concentration of neutral molecule X. X_i denotes an ion at which X is detected. If X is detected at several different ions, as is the case for SA, the signals are summed.

Calibration coefficients for sulphuric acid range from 1×10^9 to 2×10^{10} cm^{-3}, depending also on the length of the inlet tube (Berndt et al., 2015; Jokinen et al., 2012). Alternative methods, such as gravimetric perfluoroheptanoic acid calibration, have also been applied resulting in calibration coefficient of 1.6×10^{10} cm^{-3} (Ehn et al., 2014). The estimated uncertainty of the final concentrations is large, typically -50/+100 % (Ehn et al., 2014; Jokinen et al., 2014; Kirkby et al., 2016). Provided the constant sampling and instrumental conditions are maintained, the precision in determined concentration is less than 10 % (Ehn et al., 2014), allowing tracking variations in time with high confidence.

Limit of detection

In mass spectrometry, the theoretic limit of detection (LOD) will depend on the detection efficiency and on the background noise and, hence, on the averaging time (Jokinen et al., 2012, M. Ehn and C. Yan, personal communication, August 13, 2020). LOD will be always compound- and instrument-specific. The theoretical LOD is commonly determined as three standard deviations of the noise, to which calibration coefficient has been applied (Jokinen et al., 2012). This definition is also applied in **Paper V**. As the detection efficiency of most other compounds is currently unknown, the LOD can be only a rough estimation.

The real LOD will in addition depend on the interference from other compounds that are detected at the same unit m/z (**Paper III**). An example is shown for SA and SA-DMA clusters in Figure 5. Figure 5 shows 1-hour averaged spectral peaks around midday during four NPF events in Shanghai (**Paper III**). For all three clusters of

interest (marked in pink in Figure 5), the abundance of neighbouring compounds affects LOD. For $H_2SO_4 \cdot HSO_4^-$ cluster, this effect is least important as this cluster dominates the signal at that mass. In contrast for other two clusters, the signals are masked by the neighbouring peaks. The real LOD will be also time-dependent. During days when interfering peak is further away from the cluster, LOD will be lower. On days, such as 4th of December 2015 (first row, second and third columns in Figure 5), clusters of interest are located at the shoulder of the interfering peak and their LOD will be higher. Such effect on real LOD is difficult to quantify as it will vary in time and will depend on the resolving power of the TOF mass spectrometer in use.

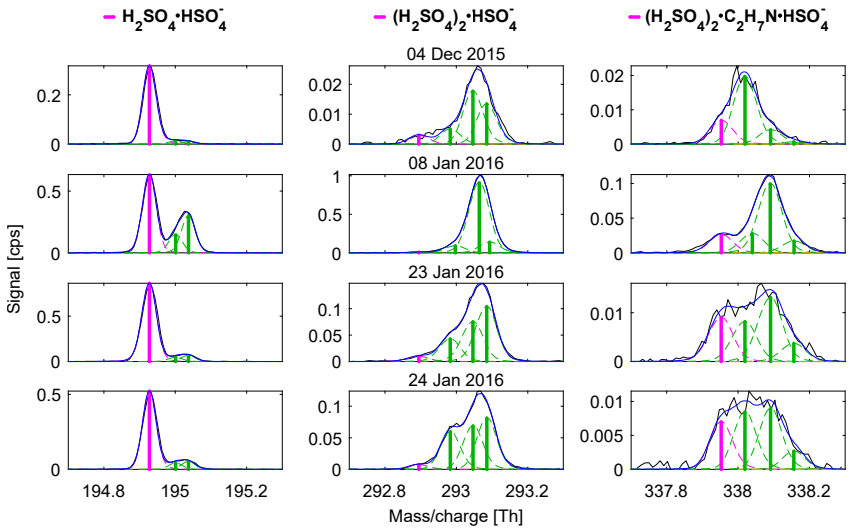

Figure 5: The figure shows the fitted peaks for sulphuric acid dimer, trimer and SA-DMA cluster in pink and interfering compounds at the same m/z in green. X-axis presents m/z and y-axis shows signal in counts per second. Each row of figures represent a specific day, which is indicated on y-axis label. Figure adapted from **Paper III** and reprinted with permission from AAAS.

3.1.3 Other Instrumentation

Integral part of my thesis were the measurements of aerosol particle size distribution. The particle number size distribution below 3 nm in diameter was measured using

Particle Size Magnifier (PSM; Vanhanen et al., 2011). Differential mobility particle sizer (DMPS) or scanning mobility particle sizer (SMPS) was used for inferring particle number size distribution from 3 nm to approximately 1 μm (Aalto et al., 2001) as well as calculating CS. The number size distribution of ions and particles between ca. 0.8 and 40 nm was measured by Neutral Air Ion Spectrometer (NAIS; Mirme & Mirme, 2013).

Aerosol chemical composition in **Paper IV** was inferred from Aerosol Mass Spectrometer (AMS, DeCarlo 2006). In addition, proton transfer reaction mass spectrometer (PTR-MS) was utilized to detect the concentration of VOC in **Paper IV**.

3.2 Atmospheric studies

In order to meet the objectives 1 and 2 of this thesis, we conducted ambient atmospheric measurement. We sampled near-ground air in the rural boreal forest as well as in a heavily polluted megacity.

The measurements at the boreal forest in **Paper I**, **II** and **V** were conducted at the Station for Measuring Ecosystem-Atmosphere Relations (SMEAR II). SMEAR II station is located in Hyytiälä in Southern Finland and represents a rural managed forest site (Hari & Kulmala, 2005). The area around the station is covered in homogeneous forest with Scots pine (*Pinus sylvestris*) as the the most abundant tree species, which is characterised by dominant monoterpene emissions (Hakola et al., 2006). The measurements were located inside of the forest canopy and conducted in spring time, when the emissions of VOC are largest and new particle formation is most frequent (Aalto et al., 2015; Nieminen et al., 2014).

The measurements at an urban site in **Paper III** were conducted in a Chinese megacity Shanghai. The instruments were sampling at the monitoring site of the Fudan University, which is located at the rooftop, about 20 m above the ground. The site is a representative urban site influenced by one of the main highways located about 100 m away as well as by industrial and residential activities in the area (**Paper III**).

3.3 Laboratory studies

To support atmospheric observations, we have conducted laboratory experiments aimed at studying the oxidation of different VOC and the formation of HOM (objective 3 of the thesis). The experiments took place at the University of Helsinki, Finland, as well as Research Centre Jülich, Gemany.

Laboratory experiments were conducted using two different set-ups: flow reactor (**Papers IV** and **V**) and atmospheric chamber (**Paper IV**). Flow reactors allow sampling first steps of oxidation at short residence times. In contrast, in chamber, simulations of longer atmospheric lifetimes and SOA formation are possible. The combination of both experimental set-ups helped us to simulate atmospheric processes occurring at different time scales.

Flow reactor experiments took place at the University of Helsinki. The set up used in **Paper IV** is shown in Figure 6. Reactants were fed into the 2 m long flow reactor. Water photolysis at 184.9 nm was used to produce OH radicals. To be able to pass the UV light, flow reactor was made of quartz. VOC was fed in by bubbling nitrogen (N_2) through a liquid VOC or by passing nitrogen over, in case the VOC was solid at room temperature. The oxidation products were sampled by CI-APi-TOF positioned as close as possible and in alignment with the flow reactor. This positioning ensured minimal losses of HOM. The flow rate was regulated by CI-APi-TOF, and was about 12 lpm in total, moderating the residence time in the reactor to 10 s.

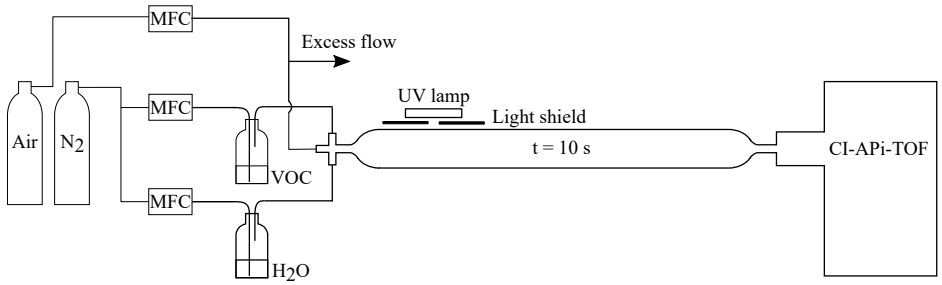

Figure 6: The flow reactor set-up. Figure is from **Paper IV**.

For experiments in **Paper V**, the flow reactor was made from borosilicate glass and the set-up was modified so that, instead of water, ozone was fed to the flow reactor. Ozone

was produced prior to entering the flow reactor by oxygen photolysis at 184.9 nm light. The oxidation was conducted in dark conditions. The residence time was maintained at 18 s.

Chamber experiments in **Paper IV** took place in Jülich Plant Atmosphere Chamber (JPAC) at the Research Centre Jülich, Germany (Mentel et al., 2009), which is made of borosilicate glass. The residence time was set to 48 min. OH there was produced from ozone photolysis at 254 nm in presence of water. VOC was fed by flowing N_2 through a diffusion source. Ozone was guided in separately from VOC and in the same line as water vapour. The CI-APi-TOF was located directly under the chamber with a straight inlet sampling the chamber air.

4 Results and discussion

4.1 Aerosol precursors in boreal forest

New particle formation as a regional phenomenon was confirmed at SMEAR II station located in Hyytiälä in the Finnish Boreal forest around 20 years ago (Mäkelä et al., 1997). Since then, continuous measurement allowed the conclusion that NPF happened preferentially in spring and in the autumn during the day time and at higher solar insolation, lower CS and clean North air masses (Nieminen et al., 2014; Dada et al., 2017, and references therein). Indirectly, it was clear that sulphuric acid and organics play a role in NPF, but exact clustering pathways remained unknown (Riipinen et al., 2011; Kulmala et al., 2013).

With the development of an APi-TOF, it was possible to measure the freshly formed clusters, SA and HOM. According to current knowledge, mainly ammonia, and not dimethylamine, acts as a stabilizer for clusters at SMEAR II (Schobesberger et al., 2015; Sipilä et al., 2015; Lehtipalo et al., 2018). Ammonia-SA system tends to have lower particle formation rates, which are enhanced by the presence of ions (Kirkby et al., 2011). It also was clear that HOM must participate in either clustering or growth of those clusters (Kulmala 2013). While ion-induced nucleation can only account for about 10% of total particles formed at the site (Manninen et al., 2009a), ions can stabilize molecular clusters and have a significant effect on particle formation rates (Kirkby et al., 2011; Kirkby et al., 2016). In **Papers I and II**, we determine the relationship between the availability of electrically neutral low-volatility vapours and the composition of negatively charged clusters as well as investigate the clustering pathway responsible for ion-induced particle formation at the SMEAR II station.

4.1.1 The role of HOM and SA in naturally charged ions

In **Paper I**, we examined the composition and diel evolution of natural negatively charged HOM clusters and compared them to the SA-bisulphate clusters, neutral SA as well as neutral HOM profiles. The measurements took place during the spring, when the emissions of biogenic VOC is largest (Aalto et al., 2015). In the analysis, we considered only sunny days, as radiation controls the daytime evolution of SA. Figure 7 presents negative ions and neutral molecules divided into groups based on

their composition for a representative day and night in mass defect plots. Mass defect is the difference between the nominal mass of an ion (here defined as the nearest integer mass) and its exact mass, a parameter that allows identification of compounds that appear at the same unit m/z. Each coloured circle on Figure 7 represents a unique chemical composition of an identified ion, while open circles show unidentified peaks.

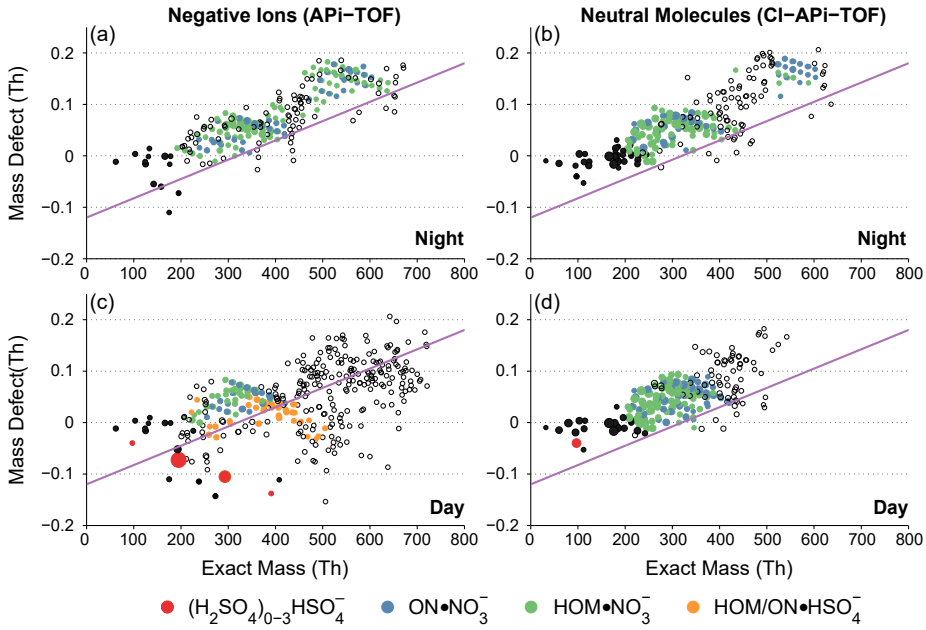

Figure 7: Detected negative ions and neutral molecules during night and day as measured by APi-TOF (panels a and c) and CI-APi-TOF (panels b and d) in SMEAR II station on April 20, 2013. The size of the circles is logarithmically proportional to the observed signal, and scale is different among instruments. Open circles indicate unidentified peaks. Figure is from **Paper I**.

During the night (panels a and b on Figure 7), the composition of ionic HOM detected by APi-TOF was very similar to neutral compounds detected by CI-APi-TOF. The reason is that, at night, nitrate is naturally the primary ion to cluster with HOM, which is equivalent to artificial ionisation in CI-APi-TOF. Two bands of HOM were present in both instrument: monomers (250–450 m/z) and dimers (450–650 m/z). During night, nitrogen-containing HOM likely formed in nitrate radical oxidation of monoterpenes,

while HOM with no nitrogen primarily formed in monoterpene ozonolysis (Ehn et al., 2014; Yan et al., 2016).

In contrast with nigh time, solar radiation during the day facilitated SA formation. SA is a strong acid, which will easily donate a proton and form a bisulphate. Bisulphate ions and its clusters with neutral SA molecules dominated the negative ions during the day, as seen in panel c of Figure 7 marked in red colour. The presence of bisulphate in the air was competing with nitrate ion for forming clusters with HOM molecules. As a result, the detected compounds in APi-TOF and CI-APi-TOF were very different (panels c and d on Figure 7). It was for the first time that HOM-bisulphate clusters were identified during the day time at SMEAR II. Some of these clusters were also seen in alpine environment (Bianchi et al., 2016). In the laboratory, these clusters were identified in CLOUD experiment, in which SA nucleation in presence of oxidised organics was studied (Schobesberger et al., 2013; Riccobono et al., 2014). Therefore, it is likely that the HOM-bisulphate clusters can explain a fraction of ion-induced clustering and particle formation at SMEAR II station.

The abundance of NO in the daytime (particularly during morning hours) induced further differences in the product distribution. Similarly to night, we also observed nitrogen-containing HOM during the day, but their formation likely involved termination of autoxidation by NO (Yan et al., 2016). Another difference during day time was that dimers were far less abundant in CI-APi-TOF, in comparison to night, which can also be explained by NO terminating autoxidation and reducing the amount of available RO_2 radicals for dimer formation. It must be mentioned that it is likely that the spectrum looks different in other seasons. For instance, Zhang et al. (2020) recently identified daytime dimers in autumn.

It was impossible to identify the atomic composition of negatively charged clusters in APi-TOF that were found in the dimer region during the day (open circles in Figure 7, panel c). The identification of masses above ca. 450 m/z is limited by the instrumental resolving power, lower concentration of dimers as well as due to increased possibilities in composition assignment at larger m/z. In addition, some nitrogen-containing HOM clustered with NO_3^- may overlap on the same unit m/z with no-nitrogen containing HOM clustered with HSO_4^-. To help with assessing the chemical composition of unidentified peaks, a violet line was added to Figure 7 for guidance. The line represents the lower limit of mass defect for identified ions as clusters with NO_3^- in CI-APi-TOF. Therefore, natural ions that are located below that line at 450-650 m/z range in day

time are unlikely to be clusters with NO_3^-. We hypothesised that those negatively charged clusters are HOM dimers clustered with bisulphate. Later study on multi-component particle formation in CLOUD chamber, which was aimed at simulating SMEAR II atmosphere, confirmed this hypothesis (Lehtipalo et al., 2018).

On a different night of 13^{th} of March 2012, we also identified pure organic HOM clusters with up to 40 carbon atoms. These clusters appeared in natural ions charged by NO_3^- and resembled compounds that were observed in pure α-pinene initiated NPF studied in the CLOUD chamber (Kirkby et al., 2016). Kirkby et al. (2016) found that in pure biogenic system stabilization of clusters by ions played a crucial role in determining particle formation rates. Later on, Rose et al. (2018) showed that the same large HOM clusters initiated frequent night-time clustering events in SMEAR II station, but they did not grow to form new particles.

4.1.2 Factors driving ion-induced particle formation

In addition to naturally charged clusters of HOM and SA observed at SMEAR II station (**Paper I**), Schobesberger et al. (2013) identified sulphuric acid-ammonia (SA-NH_3) clusters during clustering events at this site. In **Paper II**, we wanted to explore how the appearance of SA-NH_3 clusters connects to new particle formation. The analysis was done for spring months during years 2011 to 2013 and combined APi-TOF, CI-APi-TOF, particle and ion size distribution measurements.

During the consecutive three springs, 67 ion-induced clustering events were observed. Each of the events is represented by a dot in Figure 8. The events could be separated by the clustering mechanisms: red dots represent days when SA-NH_3 were observed, while blue dots represent events when no SA-NH_3 clusters were observed and, instead, a negative ion spectra was dominated by HOM clusters, similar to Figure 7, panel c. The clustering pathway could be explained by the ratio between the abundance of electrically neutral HOM and SA (panel a in Figure 8). When HOM-to-SA ratio was below 30, sulphuric acid and bisulphate preferentially clustered with ammonia, while at higher ratios, HOM was carrying most of the charge, as adducts with NO_3^- and HSO_4^-.

When SA content reached six molecules in the cluster, ion-induced event always occurred. During SA-NH_3 events, clusters with up to $(H_2SO_4)_{10}\cdot (NH_3)_{11}\cdot HSO_4^-$ have

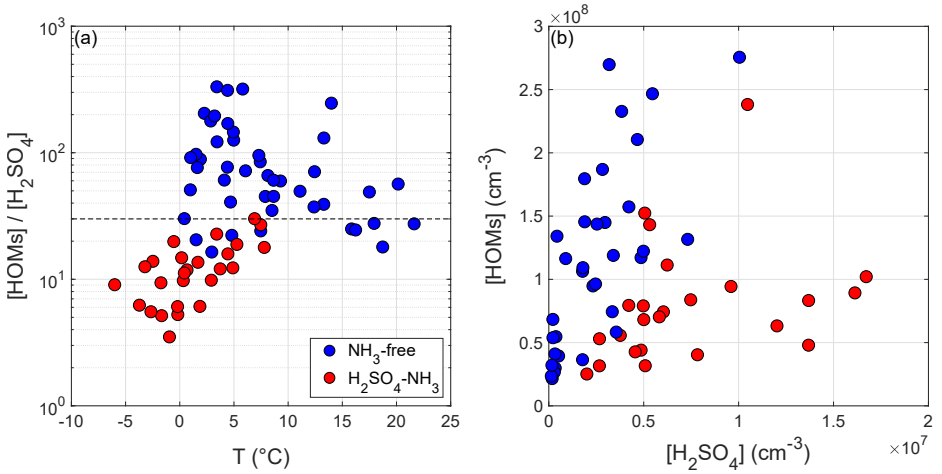

Figure 8: Factors controlling ion-induced nucleation in spring at SMEAR II station. Each dot represents an average value over one NPF event. Red dots are days with SA-NH_3 clusters observed, while blue dots are days in which no NH_3 has been detected in negative clusters. Figure is from **Paper II**.

been observed, corresponding to about 1.7 nm diameter. However, during other events, no such big clusters were seen. During those days, however, particle formation rate correlated with ionic HOM clusters, suggesting HOM are somehow involved in the formation of charged particles, as was hypothesized in **Paper I**. However, the exact role of HOM-SA ion clusters is yet to be elucidated. The clustering chemistry did not depend on the concentration of ammonia. Temperature and radiation, on the other hand, affected HOM-to-SA ratio. As a result, studies in other seasons are also needed.

While the role of ammonia has become clear in ion-induced clustering events, the neutral pathway has been unclear. Lehtipalo et al. (2018) have investigated NH_3-SA-HOM-NO_X particle formation in CLOUD chamber aiming to simulate the conditions at SMEAR II. Ions played a role at low SA concentrations and the negative ion cluster composition was similar to the one seen in **Paper I** (Figure 7c). They also confirmed that the abundance of HOM dimers controlled the initial growth of particles. Even if indirectly it is clear that the mixture of precursors can explain NPF in SMEAR II station, the exact composition of multicomponent negatively charged and neutral clusters in the range beyond 700 m/z is not possible to identify with the current techniques, though some them were seen in positive clusters (Lehtipalo et al., 2018).

4.2 NPF precursors in an urban atmosphere

Strong new particle formation (NPF) events can be observed in urban areas despite high concentrations of pre-existing particles (Kulmala et al., 2004; Kulmala et al., 2017; Kerminen et al., 2018, and references therein). In comparison to boreal forest, where 1.5–3 nm particle formation rates are typically within 0.1–1 $cm^{-3}\,s^{-1}$ (Dada et al., 2017), in urban areas they often can reach about 100 $cm^{-3}\,s^{-1}$ or more (Kuang et al., 2008; Deng et al., 2020, **Paper III**). NPF events that lead to a large number of particles, as a hypothesis, may influence the formation of haze (Guo et al., 2014). Haze poses a risk to health among large urban population. Increasing our knowledge in the pathways towards NPF in urban environments is, therefore, an important step in understanding the sources of air pollution, but also in assessing the effect of urban areas on global aerosol budget.

To understand the vapours responsible for clustering and NPF in a city, we deployed CI-APi-TOF for 3 months during winter 2015–2016 in Shanghai, China (**Paper III**). This campaign was conducted in support of continuous measurements of particle size distribution, from which a two-year NPF trend was analysed. During this period, NPF events were associated with photochemical activity and observed on 15.6 % of the days. It was clear that the clustering mainly progresses via neutral pathway as only about 1 % of particle formation rate could be explained by ions. During the intensive campaign, we detected 15 events, in 9 out of which we could measure the vapours and clusters with CI-APi-TOF.

On NPF event days, sulphuric acid (hereafter SA monomer) increased to about $10^7\,cm^{-3}$ and, at the same time, we observed a proportional increase in sulphuric acid - bisulphate ion cluster (hereafter SA dimer) (Figure 9a). SA dimer concentration on NPF days was 10^4–$10^6\,cm^{-3}$, highest ever seen in the ambient air (Kürten et al., 2016a). The particle formation rate correlated with SA dimer concentration, suggesting that the formation of the clusters that are detected as SA dimer was needed for NPF. Previous studies showed that sulphuric acid - bisulphate clusters appear in CI-APi-TOF when neutral sulphuric acid-base clusters (e.g., $(SA)_n{\cdot}(DMA)_m$) are charged with $(HNO_3)_n{\cdot}NO_3^-$ ions (Petäjä et al., 2011). Upon charging, one SA molecule is converted to a bisulphate ion. At the same time, most of base molecules will evaporate while cluster tries to reach a new stable state, and SA dimer will be formed (Ortega et al., 2014; Rondo et al., 2016). SA dimer forming at collision limit was observed

in SA-DMA-H_2O particle formation system containing atmospheric concentrations of sulphuric acid in presence of about 5 ppt of DMA (Almeida et al., 2013; Kürten et al., 2014).

As the observed particle formation rates and SA dimer-to-monomer ratio in Shanghai was high, we hypothesised that NPF during the measured period was initiated by SA-DMA-H_2O clustering. SA dimer-to-monomer ratio was higher than would be expected due to ion-induced clustering (IIC) in the CI inlet (Figure 9a), suggesting that SA dimer was not formed inside our instrument. The actual measured SA dimer-to-monomer ratio was lower than the modelled ratio for collision-limited regime. This discrepancy could be due to lower DMA concentration or other factors that differentiate ambient processes from well-controlled laboratory experiments. The lower SA dimer-to-monomer ratio in Shanghai when compared to experimental results from CLOUD chamber (Almeida et al., 2013) could be explained by the higher cluster loss rate in the ambient air (CS of about $0.02\,s^{-1}$). In comparison to NPF event days, CS on non-event days was on average larger than $0.02\,s^{-1}$, which further increased cluster losses inhibiting NPF during those days.

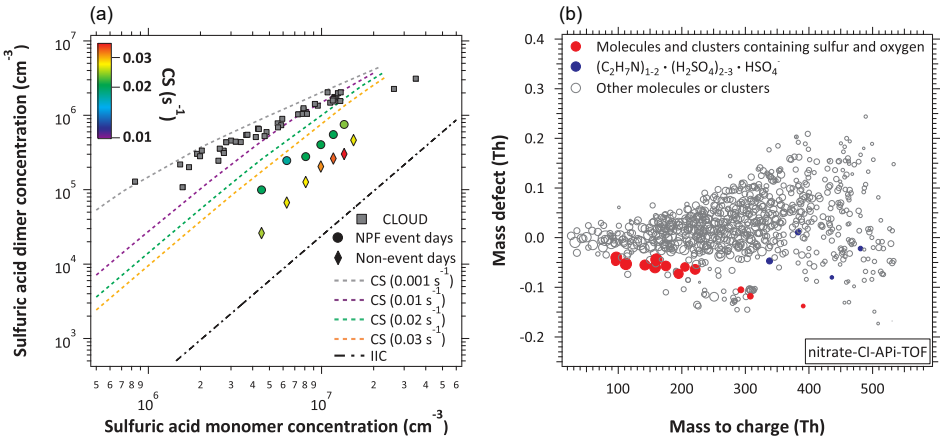

Figure 9: Comparison of the observed SA dimer-to-SA monomer ratio with model and data from CLOUD experiment (panel a) and mass defect plot of neutral clusters and molecules as observed around noon on a NPF event day in Shanghai (panel b). Reprinted from **Paper III** with permission from AAAS.

In addition to SA dimer as indicator for the abundance of neutral clusters, we also directly detected SA trimer and tetramer as well as few DMA-SA-bisulphate clusters (Figure 9b). The clusters were present at very small concentrations and their concentration peaked around noon when the particle formation rates were highest. In contrast to CLOUD SA-DMA experiments (Kürten et al., 2014), we did not observe larger clusters. CLOUD experiments are often conducted at constant supply of precursors and low CS, factors that may result in more clusters seen in the chamber. Similar SA-DMA clusters were also seen later in Beijing by Brean et al. (2019). Using a model to simulate SA-DMA cluster population, we were able to explain the observed growth of particles in Shanghai up to 3 nm in diameter via co-condensation of SA and DMA molecules. Our hypothesis that NPF in Shanghai initiated via SA-DMA clustering was, therefore, supported by several independent observations.

Besides SA-bisulphate and SA-DMA-bisulphate clusters, Figure 9b shows a large amount of other detected compounds. Identification of only few peaks was possible as we were limited by the resolving power of the CI-APi-TOF and the abundance of multiple peaks at a given unit m/z. Due to majority of peaks having a positive mass defect, we concluded that the majority of the peaks were organic compounds. High concentration of organics is expected in highly polluted atmosphere characterised by traffic and industrial emissions. In Shanghai, no clear monomer-dimer separation was seen, similar to daytime spectrum at SMEAR II station (see Figure 7d). HOM likely represent a fraction of the observed peaks, but more work is needed to identify their role in NPF. Along with other studies conducted in China, we can only hypothesise that the growth of particles beyond 3 nm in diameter is due to organic condensation.

4.3 Production of HOM in VOC oxidation

Laboratory experiments of monoterpene oxidation in JPAC chamber were crucial in confirming the origin and the composition of HOM in the boreal forest (Ehn et al., 2012). In addition, the identification of many clusters in **Papers II** and **III** relied on the results obtained in CLOUD chamber. However, a large portion of potential HOM in **Paper I** and **III** remained unidentified. To understand the sources of HOM to ambient air better, we performed experiments focusing on other important, but less studied from HOM perspective, VOC: aromatics and sesquiterpenes.

4.3.1 Anthropogenic VOC: aromatic

Aromatic VOC are the most prominent SOA precursors in urban air (Kroll & Seinfeld, 2008). They come mainly from anthropogenic activity, such as traffic, industrial emissions and solvent use. Aromatic compounds contain a six-carbon benzene ring, which is very stable due to de-localised electrons on pi-orbitals. If an aromatic compound is non-oxygenated, its reactivity is generally low, in comparison for instance to alkenes. In the atmosphere, aromatics primarily react with hydroxyl radical (OH) (Atkinson & Arey, 2003). A distinct feature of the aromatic oxidation is that the products of oxidation are much more reactive than the parent VOC, making consecutive oxidation reactions more likely than in other systems.

In **Paper IV**, we conducted a series of aromatic oxidation experiments. At first, we tested benzene (C_6H_6), toluene (C_6H_8) and naphthalene ($C_{10}H_8$) reaction with OH in a flow reactor. Interestingly, all three compounds produced very oxygenated HOM, similarly to biogenic alkenes studied before (Figure 10). The products were mainly closed-shell, majority of which we could explain with known RO_2 radical termination pathways. We detected many similar HOM products as in the studies conducted by Molteni et al. (2018) and Wang et al. (2017), though the exact product pattern differed.

A striking difference was observed between benzene HOM pattern and that of toluene and naphthalene. Benzene spectrum could be characterised by only few dominating peaks, while other spectra showed larger variability in observed products. In addition, in benzene spectrum, a clear dominance of evenly oxygenated dimers was seen, pointing that they formed from cross reactions of RO_2 radicals with either only even or only odd oxygen. This is a significant observation as either all radicals formed from single

OH oxidation step (odd oxygen RO_2) or from secondary step (even oxygen RO_2), but not from both. Furthermore, only in benzene spectrum we directly observed RO_2 radicals, and they contained an odd number of oxygen atoms. The evidence listed above pointed that, in benzene oxidation, HOM were formed upon a single OH attack, while in toluene and naphthalene experiments, many OH oxidation steps took place. The most likely reason for that were higher reactivity of toluene and naphthalene with OH as well as their lower concentration during the experiments, promoting secondary oxidation steps.

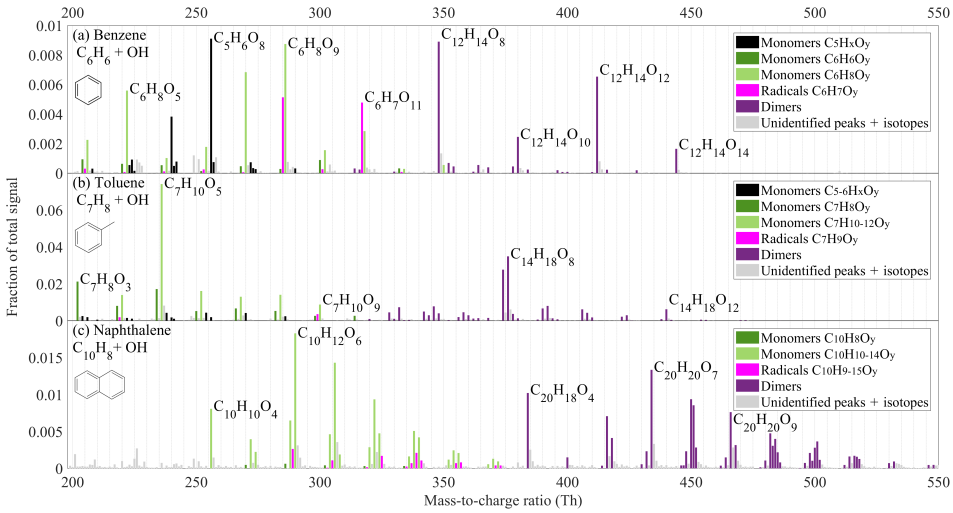

Figure 10: HOM and lower-oxygenated compounds observed in oxidation of different aromatic compounds in the flow reactor. Figure is adapted from **Paper IV**.

To further explore the effect of multiple oxidation steps on HOM formation in aromatic system, we performed a series of benzene oxidation experiments in JPAC chamber. The measured HOM molar yield increased with OH concentration about 6-fold from 1×10^7 to 4×10^8 cm^{-3} of OH (Figure 11). This confirmed that, in aromatic system, a large part of HOM forms in multiple oxidation steps. In **Paper IV**, we named such products "multi-generation HOM". Multiple oxidation reactions as source of HOM may be especially important in benzene oxidation, as substituted aromatic VOC can undergo H-shifts easier than benzene (Wang et al., 2017). While the OH concentration in our experiments were much higher than in the atmosphere, they simulate the atmospheric benzene lifetimes of several hours to several days. As HOM composition also changed

with OH exposure, taking secondary reactions into account is important in interpreting ambient observations. It is likely that some of the observed HOM will have low- or extremely low- volatilities and therefore contribute to the initial growth of particles in the urban atmosphere, such as studied in **Paper III**. Our results underlined the potential of further oxidation steps to increase HOM formation, and, therefore, have an impact on initial steps of secondary organic aerosol (SOA) formation.

Multigeneration oxidation in aromatic system was also recently studied by Schwantes et al. (2017) and Zaytsev et al. (2019), whose results pointed to the contribution of multigeneration oxidation to the formation of HOM and SOA respectively. Similar effect of multiple oxidation steps was also reported in biogenic systems by Ehn et al. (2014) and McFiggans et al. (2019), though not discussed in detail. Therefore, it is logical to conclude that HOM yield and composition from any given VOC oxidation pathway in the atmosphere will be a function of atmospheric lifetime, oxidant concentrations and loss processes.

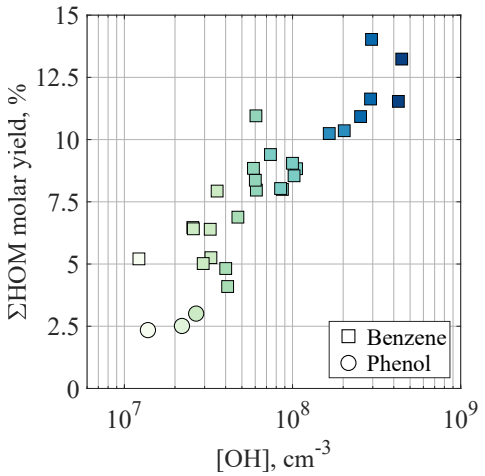

Figure 11: Increase of HOM molar yield is observed with the increase of OH concentration in benzene oxidation experiments. Colour of the dots is proportional to OH concentration. Figure adapted from **Paper IV**.

During the experiments, we also tested the effect of NO_X on HOM composition as well as added seed aerosol particles to sample the secondary organic aerosol (SOA). Upon NO_X addition, the HOM products shifted to contain nitrogen atoms, likely due

to NO and NO_2 termination of RO_2 radicals, as was reported for biogenic alkenes (Ehn et al., 2014; Yan et al., 2016; Rissanen, 2018). However, at NO_X of about 4ppb, some dimers still formed. Tsiligiannis et al. (2019) reported that the addition of NO_X to trimethylbenzene system inhibited particle formation, which is something that was previously seen in monoterpene oxidation (Wildt et al., 2014; Lehtipalo et al., 2018; Yan et al., 2020). When we added seed aerosol (in absence of NO_X), HOM condensed rapidly on the particles, which suggested that the HOM were low-volatile. However, the observed HOM consumption was faster than could be explained by irreversible condensation alone. This further strengthened our hypothesis for multi-generation HOM, as we could only explain this behaviour with the condensation of less-oxygenated compounds that would form HOM if they stayed in the gas-phase. The variability of HOM formation at different conditions may explain part of the discrepancies reported for SOA behaviour in aromatic systems in literature (Ng et al., 2007; Hildebrandt et al., 2009; Emanuelsson et al., 2013).

4.3.2 Biogenic VOC: a sequiterpene

In addition to isoprene and monoterpenes, there are myriad of other less studied VOC emitted by forests and vegetation. One of such VOC groups is sesquiterpenes, which are $C_{15}H_{24}$ molecules consisting of three isoprene units, and are comprising of about 2.5 % of global biogenic carbon emissions (Sindelarova et al., 2014). Sesquiterpenes have 1.5 times the mass of monoterpenes and some of them (for instance, β-caryophyllene, BCP) are more reactive towards ozone than monoterpenes (Hakola et al., 2012; Richters et al., 2015). Sesquiterpenes can be emitted by coniferous or broad leaf trees, wetlands as well as soil and forest floor (Duhl et al., 2008; Kajos et al., 2013; Bourtsoukidis et al., 2018; Hellén et al., 2020; Mäki, 2020). BCP is one of the dominant sesquiterpenes emitted, for instance, from Scots Pine (Hakola et al., 2006) and orange orchids (Ciccioli et al., 1999), and in **Paper V**, we have studied its potential to form HOM in the laboratory.

We found that many HOM products were formed in BCP oxidation: C_{15} monomers as well as C_{29-30} dimers. The formation of those products could be explained either by ozonolysis or by OH reactions, as OH is a byproduct of alkene reaction with O_3 (Shu & Atkinson, 1995). We estimated the lower limit of the HOM molar yield with respect to reaction with O_3 as 1.7±1.2 %. In comparison, ozonolysis of α-pinene yields about 3.4–7 % of HOM, ozonolysis of isoprene – 0.01%, and ozonolysis of limonene –

5.3–17 % (about factor of two uncertainty; Ehn et al., 2014; Jokinen et al., 2015). With similar nitrate ionisation scheme, Richters et al. (2016b) reported HOM yield of 0.5 % for BCP (factor of two uncertainty). In addition to HOM yield, using simple VBS parametrisation (Donahue et al., 2011), we estimated that HOM from β-caryophyllene are extremely low-volatile compounds. It is, therefore, possible that in some locations where sesquiterpene emissions dominate, these HOM may participate in particle formation and growth.

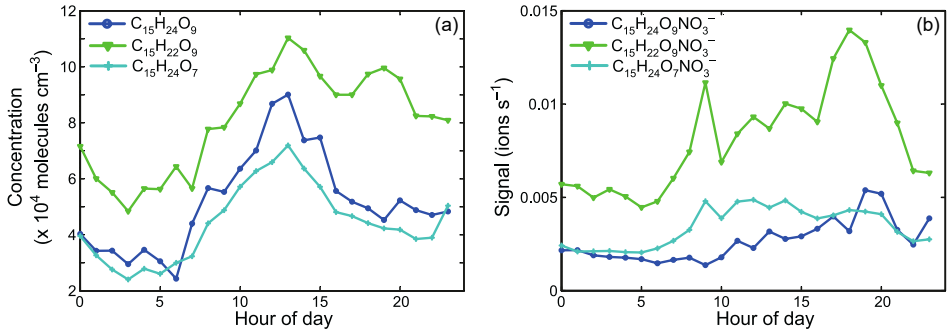

Figure 12: Diel cycle of presumed sesquiterpene-derived HOM observed in spring 2011 at SMEAR II station. Panel a shows neutral species, while panel b shows naturally charged ions. Figure adapted from **Paper V**.

To investigate if similar HOM are formed in the real atmosphere, we compared the composition of HOM from BCP oxidation to measurements at SMEAR II station. Although we could not determine if the observed HOM came from oxidation of BCP, we found HOM monomers of the same composition both in natural ions, as clusters with NO_3^-, and in electrically neutral state. Figure 12 shows the diel profiles of the detected species. The concentration of neutral HOM was very low, peaking during the day, which was similar to monoterpene-derived HOM (**Paper I**). Surprisingly, naturally-charged HOM peaked in the morning or afternoon, a pattern that among clusters with NO_3^- was only seen for nitrogen-containing C_{10} HOM (**Paper I**). Analysing field measurements from other seasons may help to confirm the presence of sesquiterpene HOM in the ambient air.

5 Review of papers and the author's contribution

Paper I investigated the effect of highly oxygenated organic molecules (HOM) and sulphuric acid (SA) on the composition of naturally charged clusters at a boreal forest site. During the night, ions mainly contained HOM clustered with nitrate ion, while in daytime, as SA concentration increased, HOM-bisulphate clusters appeared. The abundance of neutral HOM groups also was reflected in charged cluster composition. In this paper, I participated in planning and executing of the data analysis, contributed to data interpretation and writing of the manuscript.

Paper II investigated ion-induced nucleation at the same boreal forest station as in Paper I. We determined that the ratio of neutral HOM to SA governed the clustering pathway, with sulphuric acid - ammonia pathway prevailing at ratio below 30. Another pathway of daytime ion-induced nucleation events likely involved HOM ions. In this paper, I contributed to data analysis, participated in scientific discussions and commented on the manuscript.

In **Paper III**, new particle formation in Shanghai, China was studied. By comparing ambient data to previous laboratory studies, we concluded that in winter Shanghai the NPF mainly proceeds via sulphuric acid - dimethylamine clustering, co-condensation of which could also explain the growth of particles up to 3 nm. For this paper, I conducted the data analysis and interpretation, wrote part of the manuscript and supplementary as well as contributed to answering reviewer comments.

In **Paper IV**, we probed the formation of HOM in aromatic oxidation. We concluded that in our experimental conditions, HOM yield and composition depended on OH concentration. We identified multiple OH oxidation steps as an important source for total detectable HOM. I conducted flow reactor experiments, performed data analysis and interpretation and wrote a major part of the manuscript.

Paper V presents the study on HOM formation from β-caryophyllene oxidation. We explored HOM composition as well as their potential formation pathways. In addition, we found that HOM of the same composition are also measurable in the boreal forest. For this paper, I performed laboratory experiments and commented on the manuscript.

6 Conclusions and outlook

Vapours act as precursors for secondary aerosol particles in the atmosphere. To initiate the formation or growth of new particles, the vapours should be of low-volatility. The low-volatility vapours are produced in the atmosphere via oxidation reactions and can be inorganic, such as sulphuric acid (SA), and organic, such as highly oxygenated organic molecules (HOM). The growth rate will determine if a particle can reach the size of cloud condensation nuclei (CCN) instead of being lost by coagulation (Vehkamäki & Riipinen, 2012). At CCN sizes and above, particles become relevant for climate, but also potentially for other processes, such as air pollution and thereby human health. In this thesis, I investigated the vapours that can act as precursors in forming as well as growing aerosol particles in the atmosphere in different environments.

The first objective that I set for this thesis was to determine what effect the abundances of different vapours have on the composition of clusters and particles in the boreal forest. To achieve that, we looked into the natural ionic clusters at SMEAR II station in Hyytiälä, Finland (**Papers I** and **II**). We found that neutral SA, which has a maximum in concentration during the day, modified the composition of natural negatively charged HOM clusters. SA formed bisulphate ions, which took up part of HOM that otherwise were clustered with nitrate ions at night (**Paper I**). In addition, daytime abundance of SA also promoted the formation of negatively charged SA - ammonia clusters. On the days with low HOM-to-SA ratios, SA - ammonia clusters were confirmed responsible for daytime ion-induced particle formation and growth up to 3 nm (**Paper II**). However, at high HOM-to-SA ratios, another pathway was important, likely involving larger HOM - bisulphate clusters, that were proposed, but not directly identified, in **Paper I**. In both studies, HOM and SA were found to control the composition of negatively charged clusters at SMEAR II station.

The second objective of this thesis was to determine which vapours are the precursors for newly formed particles in an urban environment. This objective was achieved by the Shanghai study, in which we identified SA and dimethylamine (DMA) as precursors (**Paper III**). We could also calculate that SA-DMA co-condensation can explain the particle growth up to 3 nm in diameter. We observed a large number of potential HOM in Shanghai; however, due to instrumental limitations and high abundance of different compounds, we were unable to identify their exact chemical composition. Our hypothesis that organics, specifically HOM, drive the growth of new particles remains

to be confirmed. In **Paper III**, the measurements covered winter months and measurements from other seasons are needed to determine if other clustering mechanisms are contributing to NPF in Shanghai.

The third objective that I set was to characterise the HOM forming potential of less studied VOC, which are emitted from boreal forests and urban environments. I have fulfilled that objective by confirming that several aromatic compounds and a sesquiterpene, β-caryophyllene, can form HOM at atmospheric conditions (**Papers IV and V**). The observed HOM yields were high, though associated uncertainties were on the order of factor of two. We found that in aromatic system multi-generation oxidation will be very important for HOM formation. We also showed that aromatic-derived HOM were low-volatile, having a potential to contribute to particle growth and SOA formation in the atmosphere. While the presence of aromatic-derived HOM in ambient air is to be confirmed, a few compounds similar to β-caryophyllene-derived HOM were detected in SMEAR II station, though their concentration was very low.

The results of my thesis helped to advance our understanding in vapours that act as precursors for aerosol particles. Especially, it became clearer which vapours cluster in the boreal forest as well as in an urban environment, how the evolution of vapours changes the composition of clusters, and what is the identity and formation pathways of low-volatility vapours from oxidation of different VOC. These results may help to advance our models in order to better predict the relative impact of biogenic and anthropogenic sources of vapours to the formation of new particles and secondary organic aerosols. In addition, knowing the precursor vapours in urban environments can help in creating policies to mitigate severe air pollution episodes, such as those frequently observed in China and India. Laboratory results obtained in this thesis not only can help in future identification of vapours in ambient air, but also to advance fundamental chemical reaction pathways. As we now confirmed that HOM yield and composition is highly dependent on experimental conditions, this can be helpful in planning future experiments. Overall, the outcomes of this thesis can contribute in future field, laboratory and modelling studies.

Despite the rapid advancements in the field in recent years, including also the results of this thesis, open questions remain. While Lehtipalo et al. (2018) confirmed that multi-component NPF involving SA, ammonia, NO_X and HOM can reproduce NPF at SMEAR II station, the exact composition of neutral clusters and particles is unknown, as our current analytical tools are insufficient to measure them. Among urban

environments, we confirmed the clustering only in Shanghai so far, during the winter months. It is likely that other pathways involving ammonia and HOM are at play in different locations and seasons. In fact, an alternative theory of organic NPF has been proposed in Beijing (Guo et al., 2020a). It remains a mystery if NPF is linked to severe haze episodes, though some indication that newly formed particles increase total particle concentration during the haze has been provided (Guo et al., 2014; Kulmala et al., 2020). In addition, with our current analytical method, we are limited by the possibility to detect only molecular composition of the vapours, not their structure. Moreover, our spectra contain often thousands of species. As a result, in the future, it is imperative to develop new experimental as well as computational methods to disentangle ever-growing amounts of data. Finally, it is of utmost importance to conduct laboratory experiments in connection with field experiments, as also underlined by the results of this thesis, in order to elucidate the processes taking place in our atmosphere.

References

Aalto, J., Porcar-Castell, A., Atherton, J., Kolari, P., Pohja, T., Hari, P., Nikinmaa, E., Petäjä, T., & Bäck, J. (2015). Onset of photosynthesis in spring speeds up monoterpene synthesis and leads to emission bursts. *Plant, Cell & Environment*, *38*(11), 2299–2312. https://doi.org/10.1111/pce.12550

Aalto, P., Hämeri, K., Becker, E., Weber, R., Salm, J., Mäkelä, J. M., Hoell, C., O'Dowd, C. D., Hansson, H.-C., ... Kulmala, M. (2001). Physical characterization of aerosol particles during nucleation events. *Tellus B: Chemical and Physical Meteorology*, *53*(4), 344–358. https://doi.org/10.3402/tellusb.v53i4.17127

Albrecht, B. A. (1989). Aerosols, cloud microphysics, and fractional cloudiness. *Science*, *245*(4923), 1227–1230. https://doi.org/10.1126/science.245.4923.1227

Almeida, J., Schobesberger, S., Kürten, A., Ortega, I. K., Kupiainen-Määttä, O., Praplan, A. P., Adamov, A., Amorim, A., Bianchi, F., ... Kirkby, J. (2013). Molecular understanding of sulphuric acid–amine particle nucleation in the atmosphere. *Nature*, *502*(7471), 359–363. https://doi.org/10.1038/nature12663

Alsved, M., Fraenkel, C.-J., Bohgard, M., Widell, A., Söderlund-Strand, A., Lanbeck, P., Holmdahl, T., Isaxon, C., Gudmundsson, A., ... Löndahl, J. (2019). Sources of airborne norovirus in hospital outbreaks. *Clinical Infectious Diseases*, *70*(10), 2023–2028. https://doi.org/10.1093/cid/ciz584

Atkins, P. W. (1998). *Physical chemistry*. Oxford New York, Oxford University Press.

Atkinson, R., & Arey, J. (2003). Atmospheric degradation of volatile organic compounds. *Chemical Reviews*, *103*(12), 4605–4638. https://doi.org/10.1021/cr0206420

Atkinson, R., & Aschmann, S. M. (1989). Rate constants for the gas-phase reactions of the oh radical with a series of aromatic hydrocarbons at 296 K. *International Journal of Chemical Kinetics*, *21*(5), 355–365. https://doi.org/10.1002/kin.550210506

Baker, A. K., Beyersdorf, A. J., Doezema, L. A., Katzenstein, A., Meinardi, S., Simpson, I. J., Blake, D. R., & Rowland, F. S. (2008). Measurements of nonmethane hydrocarbons in 28 United States cities. *Atmospheric Environment*, *42*(1), 170–182. https://doi.org/10.1016/j.atmosenv.2007.09.007

Ball, S. M., Hanson, D. R., Eisele, F. L., & McMurry, P. H. (1999). Laboratory studies of particle nucleation: Initial results for H_2SO_4, H_2O, and NH_3 vapors. *Journal of*

Geophysical Research: Atmospheres, *104*(D19), 23709–23718. https://doi.org/10.1029/1999jd900411

Berndt, T., Richters, S., Jokinen, T., Hyttinen, N., Kurtén, T., Otkjær, R. V., Kjaergaard, H. G., Stratmann, F., Herrmann, H., ... Ehn, M. (2016). Hydroxyl radical-induced formation of highly oxidized organic compounds. *Nature Communications*, *7*(1). https://doi.org/10.1038/ncomms13677

Berndt, T., Richters, S., Kaethner, R., Voigtländer, J., Stratmann, F., Sipilä, M., Kulmala, M., & Herrmann, H. (2015). Gas-phase ozonolysis of cycloalkenes: Formation of highly oxidized RO_2 radicals and their reactions with NO, NO_2, SO_2, and other RO_2 radicals. *The Journal of Physical Chemistry A*, *119*(41), 10336–10348. https://doi.org/10.1021/acs.jpca.5b07295

Bianchi, F., Kurtén, T., Riva, M., Mohr, C., Rissanen, M. P., Roldin, P., Berndt, T., Crounse, J. D., Wennberg, P. O., ... Ehn, M. (2019). Highly oxygenated organic molecules (HOM) from gas-phase autoxidation involving peroxy radicals: A key contributor to atmospheric aerosol. *Chemical Reviews*, *119*(6), 3472–3509. https://doi.org/10.1021/acs.chemrev.8b00395

Bianchi, F., Praplan, A. P., Sarnela, N., Dommen, J., Kürten, A., Ortega, I. K., Schobesberger, S., Junninen, H., Simon, M., ... Baltensperger, U. (2014). Insight into acid–base nucleation experiments by comparison of the chemical composition of positive, negative, and neutral clusters. *Environmental Science & Technology*, *48*(23), 13675–13684. https://doi.org/10.1021/es502380b

Bianchi, F., Trostl, J., Junninen, H., Frege, C., Henne, S., Hoyle, C. R., Molteni, U., Herrmann, E., Adamov, A., ... Baltensperger, U. (2016). New particle formation in the free troposphere: A question of chemistry and timing. *Science*, *352*(6289), 1109–1112. https://doi.org/10.1126/science.aad5456

Bourtsoukidis, E., Behrendt, T., Yañez-Serrano, A. M., Hellén, H., Diamantopoulos, E., Catão, E., Ashworth, K., Pozzer, A., Quesada, C. A., ... Williams, J. (2018). Strong sesquiterpene emissions from Amazonian soils. *Nature Communications*, *9*(1). https://doi.org/10.1038/s41467-018-04658-y

Boy, M., Kulmala, M., Ruuskanen, T. M., Pihlatie, M., Reissell, A., Aalto, P. P., Keronen, P., Maso, M. D., Hellen, H., ... Arnold, F. (2005). Sulphuric acid closure and contribution to nucleation mode particle growth. *Atmospheric Chemistry and Physics*, *5*(4), 863–878. https://doi.org/10.5194/acp-5-863-2005

Brean, J., Beddows, D. C. S., Shi, Z., Temime-Roussel, B., Marchand, N., Querol, X., Alastuey, A., Minguillón, M. C., & Harrison, R. M. (2020). Molecular insights into new particle formation in Barcelona, Spain. *Atmospheric Chemistry and Physics*, *20*(16), 10029–10045. https://doi.org/10.5194/acp-20-10029-2020

Brean, J., Harrison, R. M., Shi, Z., Beddows, D. C. S., Acton, W. J. F., Hewitt, C. N., Squires, F. A., & Lee, J. (2019). Observations of highly oxidized molecules and particle nucleation in the atmosphere of Beijing. *Atmospheric Chemistry and Physics*, *19*(23), 14933–14947. https://doi.org/10.5194/acp-19-14933-2019

Ciccioli, P., Brancaleoni, E., Frattoni, M., Palo, V. D., Valentini, R., Tirone, G., Seufert, G., Bertin, N., Hansen, U., ... Sharma, M. (1999). Emission of reactive terpene compounds from orange orchards and their removal by within-canopy processes. *Journal of Geophysical Research: Atmospheres*, *104*(D7), 8077–8094. https://doi.org/10.1029/1998jd100026

Coffman, D. J., & Hegg, D. A. (1995). A preliminary study of the effect of ammonia on particle nucleation in the marine boundary layer. *Journal of Geophysical Research*, *100*(D4), 7147–7160. https://doi.org/10.1029/94jd03253

Crounse, J. D., Knap, H. C., Ørnsø, K. B., Jørgensen, S., Paulot, F., Kjaergaard, H. G., & Wennberg, P. O. (2012). Atmospheric fate of methacrolein. 1. peroxy radical isomerization following addition of OH and O_2. *The Journal of Physical Chemistry A*, *116*(24), 5756–5762. https://doi.org/10.1021/jp211560u

Crounse, J. D., Nielsen, L. B., Jørgensen, S., Kjaergaard, H. G., & Wennberg, P. O. (2013). Autoxidation of organic compounds in the atmosphere. *The Journal of Physical Chemistry Letters*, *4*(20), 3513–3520. https://doi.org/10.1021/jz4019207

Dada, L., Paasonen, P., Nieminen, T., Mazon, S. B., Kontkanen, J., Peräkylä, O., Lehtipalo, K., Hussein, T., Petäjä, T., ... Kulmala, M. (2017). Long-term analysis of clear-sky new particle formation events and nonevents in Hyytiälä. *Atmospheric Chemistry and Physics*, *17*(10), 6227–6241. https://doi.org/10.5194/acp-17-6227-2017

Deng, C., Fu, Y., Dada, L., Yan, C., Cai, R., Yang, D., Zhou, Y., Yin, R., Lu, Y., ... Jiang, J. (2020). Seasonal characteristics of new particle formation and growth in urban Beijing. *Environmental Science & Technology*, *54*(14), 8547–8557. https://doi.org/10.1021/acs.est.0c00808

Dockery, D. W., & Pope, C. A. (1994). Acute respiratory effects of particulate air pollution. *Annual Review of Public Health*, *15*(1), 107–132. https://doi.org/10.1146/annurev.pu.15.050194.000543

Donahue, N. M., Epstein, S. A., Pandis, S. N., & Robinson, A. L. (2011). A two-dimensional volatility basis set: 1. organic-aerosol mixing thermodynamics. *Atmospheric Chemistry and Physics*, *11*(7), 3303–3318. https://doi.org/10.5194/acp-11-3303-2011

Duhl, T. R., Helmig, D., & Guenther, A. (2008). Sesquiterpene emissions from vegetation: A review. *Biogeosciences*, *5*(3), 761–777. https://doi.org/10.5194/bg-5-761-2008

Ehn, M., Junninen, H., Petäjä, T., Kurtén, T., Kerminen, V.-M., Schobesberger, S., Manninen, H. E., Ortega, I. K., Vehkamäki, H., ... Worsnop, D. R. (2010). Composition and temporal behavior of ambient ions in the boreal forest. *Atmospheric Chemistry and Physics*, *10*(17), 8513–8530. https://doi.org/10.5194/acp-10-8513-2010

Ehn, M., Kleist, E., Junninen, H., Petäjä, T., Lönn, G., Schobesberger, S., Dal Maso, M., Trimborn, A., Kulmala, M., ... Mentel, T. F. (2012). Gas phase formation of extremely oxidized pinene reaction products in chamber and ambient air. *Atmospheric Chemistry and Physics*, *12*(11), 5113–5127. https://doi.org/10.5194/acp-12-5113-2012

Ehn, M., Thornton, J. A., Kleist, E., Sipilä, M., Junninen, H., Pullinen, I., Springer, M., Rubach, F., Tillmann, R., ... Mentel, T. F. (2014). A large source of low-volatility secondary organic aerosol. *Nature*, *506*(7489), 476–479. https://doi.org/10.1038/nature13032

Eisele, F. L. (1989a). Natural and anthropogenic negative ions in the troposphere. *Journal of Geophysical Research*, *94*(D2), 2183. https://doi.org/10.1029/jd094id02p02183

Eisele, F. L. (1989b). Natural and transmission line produced positive ions. *Journal of Geophysical Research*, *94*(D5), 6309. https://doi.org/10.1029/jd094id05p06309

Eisele, F. L., & Tanner, D. J. (1993). Measurement of the gas phase concentration of H_2SO_4 and methane sulfonic acid and estimates of H_2SO_4 production and loss in the atmosphere. *Journal of Geophysical Research: Atmospheres*, *98*(D5), 9001–9010. https://doi.org/10.1029/93jd00031

Emanuelsson, E. U., Hallquist, M., Kristensen, K., Glasius, M., Bohn, B., Fuchs, H., Kammer, B., Kiendler-Scharr, A., Nehr, S., ... Mentel, T. F. (2013). Formation of anthropogenic secondary organic aerosol (SOA) and its influence on biogenic SOA properties. *Atmospheric Chemistry and Physics*, *13*(5), 2837–2855. https://doi.org/10.5194/acp-13-2837-2013

Fang, X., Hu, M., Shang, D., Tang, R., Shi, L., Olenius, T., Wang, Y., Wang, H., Zhang, Z., ... Guo, S. (2020). Observational evidence for the involvement of dicarboxylic acids in particle nucleation. *Environmental Science & Technology Letters*, *7*(6), 388–394. https://doi.org/10.1021/acs.estlett.0c00270

Finlayson-Pitts, B. J., & Pitts, J. N. J. (2000). *Chemistry of the upper and lower atmosphere: Theory, experiments, and applications*. Academic Press.

Frege, C., Bianchi, F., Molteni, U., Tröstl, J., Junninen, H., Henne, S., Sipilä, M., Herrmann, E., Rossi, M. J., ... Dommen, J. (2017). Chemical characterization of atmospheric ions at the high altitude research station Jungfraujoch (Switzerland). *Atmospheric Chemistry and Physics*, *17*(4), 2613–2629. https://doi.org/10.5194/acp-17-2613-2017

Frege, C., Ortega, I. K., Rissanen, M. P., Praplan, A. P., Steiner, G., Heinritzi, M., Ahonen, L., Amorim, A., Bernhammer, A.-K., ... Baltensperger, U. (2018). Influence of temperature on the molecular composition of ions and charged clusters during pure biogenic nucleation. *Atmospheric Chemistry and Physics*, *18*(1), 65–79. https://doi.org/10.5194/acp-18-65-2018

Fuller, E. N., Schettler, P. D., & Giddings, J. C. (1966). New method for prediction of binary gas-phase diffusion coefficients. *Industrial & Engineering Chemistry*, *58*(5), 18–27. https://doi.org/10.1021/ie50677a007

Fuzzi, S., Baltensperger, U., Carslaw, K., Decesari, S., van der Gon, H. D., Facchini, M. C., Fowler, D., Koren, I., Langford, B., ... Gilardoni, S. (2015). Particulate matter, air quality and climate: Lessons learned and future needs. *Atmospheric Chemistry and Physics*, *15*(14), 8217–8299. https://doi.org/10.5194/acp-15-8217-2015

Gordon, H., Kirkby, J., Baltensperger, U., Bianchi, F., Breitenlechner, M., Curtius, J., Dias, A., Dommen, J., Donahue, N. M., ... Carslaw, K. S. (2017). Causes and importance of new particle formation in the present-day and preindustrial atmospheres. *Journal of Geophysical Research: Atmospheres*, *122*(16), 8739–8760. https://doi.org/10.1002/2017jd026844

Guenther, A. (2000). Natural emissions of non-methane volatile organic compounds, carbon monoxide, and oxides of nitrogen from North America. *Atmospheric Environment*, *34*(12-14), 2205–2230. https://doi.org/10.1016/s1352-2310(99)00465-3

Guenther, A., Hewitt, C. N., Erickson, D., Fall, R., Geron, C., Graedel, T., Harley, P., Klinger, L., Lerdau, M., ... Zimmerman, P. (1995). A global model of natural volatile organic compound emissions. *Journal of Geophysical Research*, *100*(D5), 8873. https://doi.org/10.1029/94jd02950

Guo, S., Hu, M., Zamora, M. L., Peng, J., Shang, D., Zheng, J., Du, Z., Wu, Z., Shao, M., ... Zhang, R. (2014). Elucidating severe urban haze formation in china. *Proceedings of the National Academy of Sciences*, *111*(49), 17373–17378. https://doi.org/10.1073/pnas.1419604111

Guo, S., Hu, M., Peng, J., Wu, Z., Zamora, M. L., Shang, D., Du, Z., Zheng, J., Fang, X., ... Zhang, R. (2020a). Remarkable nucleation and growth of ultrafine particles from vehicular exhaust. *Proceedings of the National Academy of Sciences*, *117*(7), 3427–3432. https://doi.org/10.1073/pnas.1916366117

Guo, Y., Yan, C., Li, C., Feng, Z., Zhou, Y., Lin, Z., Dada, L., Stolzenburg, D., Yin, R., ... Kulmala, M. (2020b). Formation of nighttime sulfuric acid from the ozonolysis of alkenes in Beijing. *Atmospheric Chemistry and Physics Discussions*, *2020*, 1–18. https://doi.org/10.5194/acp-2019-1111

Hakola, H., Hellén, H., Hemmilä, M., Rinne, J., & Kulmala, M. (2012). In situ measurements of volatile organic compounds in a boreal forest. *Atmospheric Chemistry and Physics*, *12*(23), 11665–11678. https://doi.org/10.5194/acp-12-11665-2012

Hakola, H., Tarvainen, V., Bäck, J., Ranta, H., Bonn, B., Rinne, J., & Kulmala, M. (2006). Seasonal variation of mono- and sesquiterpene emission rates of scots pine. *Biogeosciences*, *3*(1), 93–101. https://doi.org/10.5194/bg-3-93-2006

Hallquist, M., Wenger, J. C., Baltensperger, U., Rudich, Y., Simpson, D., Claeys, M., Dommen, J., Donahue, N. M., George, C., ... Wildt, J. (2009). The formation, properties and impact of secondary organic aerosol: Current and emerging issues. *Atmospheric Chemistry and Physics*, *9*(14), 5155–5236. https://doi.org/10.5194/acp-9-5155-2009

Hari, P., & Kulmala, M. (2005). Station for measuring ecosystem-atmosphere relations (Smear II). *Boreal Environment Research*, *10*(5), 315–322.

Heinritzi, M., Dada, L., Simon, M., Stolzenburg, D., Wagner, A. C., Fischer, L., Ahonen, L. R., Amanatidis, S., Baalbaki, R., ... Curtius, J. (2020). Molecular understanding of the suppression of new-particle formation by isoprene. *Atmospheric Chemistry and Physics Discussions*, *2020*, 1–18. https://doi.org/10.5194/acp-2020-51

Hellén, H., Schallhart, S., Praplan, A. P., Tykkä, T., Aurela, M., Lohila, A., & Hakola, H. (2020). Sesquiterpenes dominate monoterpenes in northern wetland emissions. *Atmospheric Chemistry and Physics*, *20*(11), 7021–7034. https://doi.org/10.5194/acp-20-7021-2020

Hildebrandt, L., Donahue, N. M., & Pandis, S. N. (2009). High formation of secondary organic aerosol from the photo-oxidation of toluene. *Atmospheric Chemistry and Physics*, *9*(9), 2973–2986. https://doi.org/10.5194/acp-9-2973-2009

Hinds, W. (1999). *Aerosol technology : Properties, behavior, and measurement of airborne particles*. New York, Wiley.

Hirsikko, A., Laakso, L., Horrak, U., Aalto, P., Kerminen, V., & Kulmala, M. (2005). Annual and size dependent variation of growth rates and ion concentrations in boreal forest. *Boreal Environment Research*, *10*(5), 357–369.

Hirsikko, A., Nieminen, T., Gagné, S., Lehtipalo, K., Manninen, H. E., Ehn, M., Hõrrak, U., Kerminen, V.-M., Laakso, L., ... Kulmala, M. (2011). Atmospheric ions and nucleation: A review of observations. *Atmospheric Chemistry and Physics*, *11*(2), 767–798. https://doi.org/10.5194/acp-11-767-2011

Holloway, A. (2010). *Atmospheric chemistry*. Cambridge, RSC Pub.

Holton, J. (2003). *Encyclopedia of atmospheric sciences*. Amsterdam Boston, Academic Press.

Hõrrak, U., Salm, J., & Tammet, H. (2000). Statistical characterization of air ion mobility spectra at Tahkuse Observatory: Classification of air ions. *Journal of Geophysical Research: Atmospheres*, *105*(D7), 9291–9302. https://doi.org/10.1029/1999jd901197

Hyttinen, N., Kupiainen-Määttä, O., Rissanen, M. P., Muuronen, M., Ehn, M., & Kurtén, T. (2015). Modeling the charging of highly oxidized cyclohexene ozonolysis products using nitrate-based chemical ionization. *The Journal of Physical Chemistry A*, *119*(24), 6339–6345. https://doi.org/10.1021/acs.jpca.5b01818

Hyttinen, N., Otkjær, R. V., Iyer, S., Kjaergaard, H. G., Rissanen, M. P., Wennberg, P. O., & Kurtén, T. (2018). Computational comparison of different reagent ions in the chemical ionization of oxidized multifunctional compounds. *The Journal of Physical Chemistry A*, *122*(1), 269–279. https://doi.org/10.1021/acs.jpca.7b10015

Hyttinen, N., Rissanen, M. P., & Kurtén, T. (2017). Computational comparison of acetate and nitrate chemical ionization of highly oxidized cyclohexene ozonolysis intermediates and products. *The Journal of Physical Chemistry A*, *121*(10), 2172–2179. https://doi.org/10.1021/acs.jpca.6b12654

IPCC. (2013). *Climate change 2013: The physical science basis. contribution of working group i to the fifth assessment report of the intergovernmental panel on climate change*. Cambridge, United Kingdom, New York, NY, USA, Cambridge University Press. https://doi.org/10.1017/CBO9781107415324

Israelachvili, J. (2011). *Intermolecular and surface forces*. Burlington, MA, Academic Press.

Jimenez, J. L., Canagaratna, M. R., Donahue, N. M., Prevot, A. S. H., Zhang, Q., Kroll, J. H., DeCarlo, P. F., Allan, J. D., Coe, H., ... and, D. R. W. (2009). Evolution of organic aerosols in the atmosphere. *Science*, *326*(5959), 1525–1529. https://doi.org/10.1126/science.1180353

Jokinen, T., Berndt, T., Makkonen, R., Kerminen, V.-M., Junninen, H., Paasonen, P., Stratmann, F., Herrmann, H., Guenther, A. B., ... Sipilä, M. (2015). Production of extremely low volatile organic compounds from biogenic emissions: Measured yields and atmospheric implications. *Proceedings of the National Academy of Sciences*, *112*(23), 7123–7128. https://doi.org/10.1073/pnas.1423977112

Jokinen, T., Kontkanen, J., Lehtipalo, K., Manninen, H. E., Aalto, J., Porcar-Castell, A., Garmash, O., Nieminen, T., Ehn, M., ... Kulmala, M. (2017). Solar eclipse demonstrating the importance of photochemistry in new particle formation. *Scientific Reports*, *7*(1). https://doi.org/10.1038/srep45707

Jokinen, T., Sipilä, M., Junninen, H., Ehn, M., Lönn, G., Hakala, J., Petäjä, T., Mauldin, R. L., Kulmala, M., & Worsnop, D. R. (2012). Atmospheric sulphuric acid and neutral cluster measurements using CI-APi-TOF. *Atmospheric Chemistry and Physics*, *12*(9), 4117–4125. https://doi.org/10.5194/acp-12-4117-2012

Jokinen, T., Sipilä, M., Richters, S., Kerminen, V.-M., Paasonen, P., Stratmann, F., Worsnop, D., Kulmala, M., Ehn, M., ... Berndt, T. (2014). Rapid autoxidation forms highly oxidized RO_2 radicals in the atmosphere. *Angewandte Chemie International Edition*, *53*(52), 14596–14600. https://doi.org/10.1002/anie.201408566

Junninen, H. (2013). *Data cycle in atmospheric physics : From detected millivolts to understanding the atmosphere* (Thesis). University of Helsinki. http://urn.fi/URN:ISBN:978-952-5822-81-6

Junninen, H., Ehn, M., Petäjä, T., Luosujärvi, L., Kotiaho, T., Kostiainen, R., Rohner, U., Gonin, M., Fuhrer, K., ... Worsnop, D. R. (2010). A high-resolution mass spectrometer to measure atmospheric ion composition. *Atmospheric Measurement Techniques*, *3*(4), 1039–1053. https://doi.org/10.5194/amt-3-1039-2010

Kajos, M. K., Hakola, H., Holst, T., Nieminen, T., Tarvainen, V., Maximov, T., Petäjä, T., Arneth, A., & Rinne, J. (2013). Terpenoid emissions from fully grown east siberian *Larix cajanderi* trees. *Biogeosciences*, *10*(7), 4705–4719. https://doi.org/10.5194/bg-10-4705-2013

Kerminen, V.-M., Chen, X., Vakkari, V., Petäjä, T., Kulmala, M., & Bianchi, F. (2018). Atmospheric new particle formation and growth: Review of field observations. *Environmental Research Letters*, *13*(10), 103003. https://doi.org/10.1088/1748-9326/aadf3c

Kerminen, V.-M., Paramonov, M., Anttila, T., Riipinen, I., Fountoukis, C., Korhonen, H., Asmi, E., Laakso, L., Lihavainen, H., ... Petäjä, T. (2012). Cloud condensation nuclei production associated with atmospheric nucleation: A synthesis based on existing literature and new results. *Atmospheric Chemistry and Physics*, *12*(24), 12037–12059. https://doi.org/10.5194/acp-12-12037-2012

Kirkby, J., Curtius, J., Almeida, J., Dunne, E., Duplissy, J., Ehrhart, S., Franchin, A., Gagné, S., Ickes, L., ... Kulmala, M. (2011). Role of sulphuric acid, ammonia and galactic cosmic rays in atmospheric aerosol nucleation. *Nature*, *476*(7361), 429–433. https://doi.org/10.1038/nature10343

Kirkby, J., Duplissy, J., Sengupta, K., Frege, C., Gordon, H., Williamson, C., Heinritzi, M., Simon, M., Yan, C., ... Curtius, J. (2016). Ion-induced nucleation of pure biogenic particles. *Nature*, *533*(7604), 521–526. https://doi.org/10.1038/nature17953

Köhler, H. (1936). The nucleus in and the growth of hygroscopic droplets. *Trans. Faraday Soc.*, *32*(0), 1152–1161. https://doi.org/10.1039/tf9363201152

Kontkanen, J., Lehtipalo, K., Ahonen, L., Kangasluoma, J., Manninen, H. E., Hakala, J., Rose, C., Sellegri, K., Xiao, S., ... Kulmala, M. (2017). Measurements of sub-3 nm particles using a particle size magnifier in different environments: From clean mountain top to polluted megacities. *Atmospheric Chemistry and Physics*, *17*(3), 2163–2187. https://doi.org/10.5194/acp-17-2163-2017

Krechmer, J. E., Coggon, M. M., Massoli, P., Nguyen, T. B., Crounse, J. D., Hu, W., Day, D. A., Tyndall, G. S., Henze, D. K., ... Canagaratna, M. R. (2015). Formation of low volatility organic compounds and secondary organic aerosol from isoprene hydroxyhydroperoxide low-NO oxidation. *Environmental Science & Technology*, *49*(17), 10330–10339. https://doi.org/10.1021/acs.est.5b02031

Kreyling, W. G., Hirn, S., Möller, W., Schleh, C., Wenk, A., Celik, G., Lipka, J., Schäffler, M., Haberl, N., ... Semmler-Behnke, M. (2013). Air–blood barrier translocation of tracheally instilled gold nanoparticles inversely depends on particle size. *ACS Nano*, *8*(1), 222–233. https://doi.org/10.1021/nn403256v

Kroll, J. H., & Seinfeld, J. H. (2008). Chemistry of secondary organic aerosol: Formation and evolution of low-volatility organics in the atmosphere. *Atmospheric Environment*, *42*(16), 3593–3624. https://doi.org/10.1016/j.atmosenv.2008.01.003

Kuang, C., McMurry, P. H., McCormick, A. V., & Eisele, F. L. (2008). Dependence of nucleation rates on sulfuric acid vapor concentration in diverse atmospheric locations. *Journal of Geophysical Research*, *113*(D10). https://doi.org/10.1029/2007jd009253

Kulmala, M., Dada, L., Dällenbach, K., Yan, C., Stolzenburg, D., Kontkanen, J., Ezhova, E., Hakala, S., Tuovinen, S., ... Kerminen, V.-M. (2020). Is reducing new particle formation a plausible solution to mitigate particulate air pollution in beijing and other chinese megacities? *Faraday Discussions*. https://doi.org/10.1039/d0fd00078g

Kulmala, M., Kerminen, V.-M., Petäjä, T., Ding, A. J., & Wang, L. (2017). Atmospheric gas-to-particle conversion: Why NPF events are observed in megacities? *Faraday Discussions*, *200*, 271–288. https://doi.org/10.1039/c6fd00257a

Kulmala, M., Kontkanen, J., Junninen, H., Lehtipalo, K., Manninen, H. E., Nieminen, T., Petaja, T., Sipila, M., Schobesberger, S., ... Worsnop, D. R. (2013). Direct

observations of atmospheric aerosol nucleation. *Science*, *339*(6122), 943–946. https://doi.org/10.1126/science.1227385

Kulmala, M., Maso, M. D., Mäkelä, J. M., Pirjola, L., Väkevä, M., Aalto, P., Miikkulainen, P., Hämeri, K., & O'Dowd, C. D. (2001). On the formation, growth and composition of nucleation mode particles. *Tellus B*, *53*(4), 479–490. https://doi.org/10.1034/j.1600-0889.2001.530411.x

Kulmala, M., Petäjä, T., Ehn, M., Thornton, J., Sipilä, M., Worsnop, D., & Kerminen, V.-M. (2014). Chemistry of atmospheric nucleation: On the recent advances on precursor characterization and atmospheric cluster composition in connection with atmospheric new particle formation. *Annual Review of Physical Chemistry*, *65*(1), 21–37. https://doi.org/10.1146/annurev-physchem-040412-110014

Kulmala, M., Petäjä, T., Nieminen, T., Sipilä, M., Manninen, H. E., Lehtipalo, K., Maso, M. D., Aalto, P. P., Junninen, H., ... Kerminen, V.-M. (2012). Measurement of the nucleation of atmospheric aerosol particles. *Nature Protocols*, *7*(9), 1651–1667. https://doi.org/10.1038/nprot.2012.091

Kulmala, M., Vehkamäki, H., Petäjä, T., Maso, M. D., Lauri, A., Kerminen, V.-M., Birmili, W., & McMurry, P. (2004). Formation and growth rates of ultrafine atmospheric particles: A review of observations. *Journal of Aerosol Science*, *35*(2), 143–176. https://doi.org/10.1016/j.jaerosci.2003.10.003

Kulmala, M., Toivonen, A., Mäkelä, J. M., & Laaksonen, A. (1998). Analysis of the growth of nucleation mode particles observed in boreal forest. *Tellus B: Chemical and Physical Meteorology*, *50*(5), 449–462. https://doi.org/10.3402/tellusb.v50i5.16229

Kupiainen-Määttä, O. (2016). *From cluster properties to concentrations and from concentrations to cluster properties* (Thesis). University of Helsinki. http://urn.fi/URN:ISBN:978-952-7091-51-7

Kürten, A., Bergen, A., Heinritzi, M., Leiminger, M., Lorenz, V., Piel, F., Simon, M., Sitals, R., Wagner, A. C., & Curtius, J. (2016a). Observation of new particle formation and measurement of sulfuric acid, ammonia, amines and highly oxidized organic molecules at a rural site in central Germany. *Atmospheric Chemistry and Physics*, *16*(19), 12793–12813. https://doi.org/10.5194/acp-16-12793-2016

Kürten, A., Bianchi, F., Almeida, J., Kupiainen-Määttä, O., Dunne, E. M., Duplissy, J., Williamson, C., Barmet, P., Breitenlechner, M., ... Curtius, J. (2016b). Exper-

imental particle formation rates spanning tropospheric sulfuric acid and ammonia abundances, ion production rates, and temperatures. *Journal of Geophysical Research: Atmospheres*, *121*(20). https://doi.org/10.1002/2015jd023908

Kürten, A., Jokinen, T., Simon, M., Sipilä, M., Sarnela, N., Junninen, H., Adamov, A., Almeida, J., Amorim, A., ... Curtius, J. (2014). Neutral molecular cluster formation of sulfuric acid–dimethylamine observed in real time under atmospheric conditions. *Proceedings of the National Academy of Sciences*, *111*(42), 15019–15024. https://doi.org/10.1073/pnas.1404853111

Kürten, A., Rondo, L., Ehrhart, S., & Curtius, J. (2012). Calibration of a chemical ionization mass spectrometer for the measurement of gaseous sulfuric acid. *The Journal of Physical Chemistry A*, *116*(24), 6375–6386. https://doi.org/10.1021/jp212123n

Kurtén, T., Loukonen, V., Vehkamäki, H., & Kulmala, M. (2008). Amines are likely to enhance neutral and ion-induced sulfuric acid-water nucleation in the atmosphere more effectively than ammonia. *Atmospheric Chemistry and Physics*, *8*(14), 4095–4103. https://doi.org/10.5194/acp-8-4095-2008

Kurtén, T., Rissanen, M. P., Mackeprang, K., Thornton, J. A., Hyttinen, N., Jørgensen, S., Ehn, M., & Kjaergaard, H. G. (2015). Computational study of hydrogen shifts and ring-opening mechanisms in α-pinene ozonolysis products. *The Journal of Physical Chemistry A*, *119*(46), 11366–11375. https://doi.org/10.1021/acs.jpca.5b08948

Kurtén, T., Tiusanen, K., Roldin, P., Rissanen, M., Luy, J.-N., Boy, M., Ehn, M., & Donahue, N. (2016). α-pinene autoxidation products may not have extremely low saturation vapor pressures despite high O:C ratios. *The Journal of Physical Chemistry A*, *120*(16), 2569–2582. https://doi.org/10.1021/acs.jpca.6b02196

Lee, B. H., Mohr, C., Lopez-Hilfiker, F. D., Lutz, A., Hallquist, M., Lee, L., Romer, P., Cohen, R. C., Iyer, S., ... Thornton, J. A. (2016). Highly functionalized organic nitrates in the southeast United States: Contribution to secondary organic aerosol and reactive nitrogen budgets. *Proceedings of the National Academy of Sciences*, *113*(6), 1516–1521. https://doi.org/10.1073/pnas.1508108113

Lehtipalo, K., Yan, C., Dada, L., Bianchi, F., Xiao, M., Wagner, R., Stolzenburg, D., Ahonen, L. R., Amorim, A., ... Worsnop, D. R. (2018). Multicomponent new particle formation from sulfuric acid, ammonia, and biogenic vapors. *Science Advances*, *4*(12), eaau5363. https://doi.org/10.1126/sciadv.aau5363

Lelieveld, J., Evans, J. S., Fnais, M., Giannadaki, D., & Pozzer, A. (2015). The contribution of outdoor air pollution sources to premature mortality on a global scale. *Nature*, *525*(7569), 367–371. https://doi.org/10.1038/nature15371

Lewis, R., & Evans, W. (1997). *Chemistry*. Houndmills, Basingstoke, Hampshire, Macmillan Press Ltd.

Li, H., Riva, M., Rantala, P., Heikkinen, L., Daellenbach, K., Krechmer, J. E., Flaud, P.-M., Worsnop, D., Kulmala, M., ... Bianchi, F. (2020). Terpenes and their oxidation products in the French Landes forest: Insights from Vocus PTR-TOF measurements. *Atmospheric Chemistry and Physics*, *20*(4), 1941–1959. https://doi.org/10.5194/acp-20-1941-2020

Lohmann, U., & Feichter, J. (2005). Global indirect aerosol effects: A review. *Atmospheric Chemistry and Physics*, *5*(3), 715–737. https://doi.org/10.5194/acp-5-715-2005

Mäkelä, J. M., Aalto, P., Jokinen, V., Pohja, T., Nissinen, A., Palmroth, S., Markkanen, T., Seitsonen, K., Lihavainen, H., & Kulmala, M. (1997). Observations of ultrafine aerosol particle formation and growth in boreal forest. *Geophysical Research Letters*, *24*(10), 1219–1222. https://doi.org/10.1029/97gl00920

Mäki, M. (2020). *Volatile organic compound fluxes from northern forest soils* (Thesis). University of Helsinki. http://urn.fi/URN:ISBN:978-951-651-641-0

Makkonen, R., Asmi, A., Kerminen, V.-M., Boy, M., Arneth, A., Hari, P., & Kulmala, M. (2012). Air pollution control and decreasing new particle formation lead to strong climate warming. *Atmospheric Chemistry and Physics*, *12*(3), 1515–1524. https://doi.org/10.5194/acp-12-1515-2012

Manninen, H. E., Nieminen, T., Riipinen, I., Yli-Juuti, T., Gagné, S., Asmi, E., Aalto, P. P., Petäjä, T., Kerminen, V.-M., & Kulmala, M. (2009a). Charged and total particle formation and growth rates during EUCAARI 2007 campaign in Hyytiälä. *Atmospheric Chemistry and Physics*, *9*(12), 4077–4089. https://doi.org/10.5194/acp-9-4077-2009

Manninen, H. E., Petaja, T., Asmi, E., Riipinen, I., Nieminen, T., Mikkila, J., Horrak, U., Mirme, A., Mirme, S., ... Kulmala, M. (2009b). Long-term field measurements of charged and neutral clusters using neutral cluster and air ion spectrometer (nais). *Boreal Environment Research*, *14*(4), 591–605.

Massoli, P., Stark, H., Canagaratna, M. R., Krechmer, J. E., Xu, L., Ng, N. L., Mauldin, R. L., Yan, C., Kimmel, J., ... Worsnop, D. R. (2018). Ambient measurements of highly oxidized gas-phase molecules during the southern oxidant and aerosol study (SOAS) 2013. *ACS Earth and Space Chemistry*, *2*(7), 653–672. https://doi.org/10.1021/acsearthspacechem.8b00028

Mauldin III, R. L., Berndt, T., Sipilä, M., Paasonen, P., Petäjä, T., Kim, S., Kurtén, T., Stratmann, F., Kerminen, V.-M., & Kulmala, M. (2012). A new atmospherically relevant oxidant of sulphur dioxide. *Nature*, *488*(7410), 193–196. https://doi.org/10.1038/nature11278

Mauldin III, R. L., Tanner, D. J., Heath, J. A., Huebert, B. J., & Eisele, F. L. (1999). Observations of H_2SO_4 and MSA during PEM-Tropics-A. *Journal of Geophysical Research: Atmospheres*, *104*(D5), 5801–5816. https://doi.org/10.1029/98jd02612

McFiggans, G., Mentel, T. F., Wildt, J., Pullinen, I., Kang, S., Kleist, E., Schmitt, S., Springer, M., Tillmann, R., ... Kiendler-Scharr, A. (2019). Secondary organic aerosol reduced by mixture of atmospheric vapours. *Nature*, *565*(7741), 587–593. https://doi.org/10.1038/s41586-018-0871-y

Mentel, T. F., Springer, M., Ehn, M., Kleist, E., Pullinen, I., Kurtén, T., Rissanen, M., Wahner, A., & Wildt, J. (2015). Formation of highly oxidized multifunctional compounds: Autoxidation of peroxy radicals formed in the ozonolysis of alkenes – deduced from structure–product relationships. *Atmospheric Chemistry and Physics*, *15*(12), 6745–6765. https://doi.org/10.5194/acp-15-6745-2015

Mentel, T. F., Wildt, J., Kiendler-Scharr, A., Kleist, E., Tillmann, R., Maso, M. D., Fisseha, R., Hohaus, T., Spahn, H., ... Wahner, A. (2009). Photochemical production of aerosols from real plant emissions. *Atmospheric Chemistry and Physics*, *9*(13), 4387–4406. https://doi.org/10.5194/acp-9-4387-2009

Merikanto, J., Spracklen, D. V., Mann, G. W., Pickering, S. J., & Carslaw, K. S. (2009). Impact of nucleation on global CCN. *Atmospheric Chemistry and Physics*, *9*(21), 8601–8616. https://doi.org/10.5194/acp-9-8601-2009

Mirme, S., & Mirme, A. (2013). The mathematical principles and design of the NAIS – a spectrometer for the measurement of cluster ion and nanometer aerosol size distributions. *Atmospheric Measurement Techniques*, *6*(4), 1061–1071. https://doi.org/10.5194/amt-6-1061-2013

Mohr, C., Thornton, J. A., Heitto, A., Lopez-Hilfiker, F. D., Lutz, A., Riipinen, I., Hong, J., Donahue, N. M., Hallquist, M., ... Yli-Juuti, T. (2019). Molecular identification of organic vapors driving atmospheric nanoparticle growth. *Nature Communications*, *10*(1). https://doi.org/10.1038/s41467-019-12473-2

Molteni, U., Bianchi, F., Klein, F., Haddad, I. E., Frege, C., Rossi, M. J., Dommen, J., & Baltensperger, U. (2018). Formation of highly oxygenated organic molecules from aromatic compounds. *Atmospheric Chemistry and Physics*, *18*(3), 1909–1921. https://doi.org/10.5194/acp-18-1909-2018

Mutzel, A., Poulain, L., Berndt, T., Iinuma, Y., Rodigast, M., Böge, O., Richters, S., Spindler, G., Sipilä, M., ... Herrmann, H. (2015). Highly oxidized multifunctional organic compounds observed in tropospheric particles: A field and laboratory study. *Environmental Science & Technology*, *49*(13), 7754–7761. https://doi.org/10.1021/acs.est.5b00885

Ng, N. L., Kroll, J. H., Chan, A. W. H., Chhabra, P. S., Flagan, R. C., & Seinfeld, J. H. (2007). Secondary organic aerosol formation from *m*-xylene, toluene, and benzene. *Atmospheric Chemistry and Physics*, *7*(14), 3909–3922. https://doi.org/10.5194/acp-7-3909-2007

Nieminen, T., Asmi, A., Dal Maso, M., Aalto, P. P., Keronen, P., Petaja, T., Kulmala, M., & Kerminen, V.-M. (2014). Trends in atmospheric new-particle formation: 16 years of observations in a boreal-forest environment. *Boreal Environment Research*, *19*(B, SI), 191–214.

Orlando, J. J., & Tyndall, G. S. (2012). Laboratory studies of organic peroxy radical chemistry: An overview with emphasis on recent issues of atmospheric significance. *Chemical Society Reviews*, *41*(19), 6294. https://doi.org/10.1039/c2cs35166h

Ortega, I. K., Olenius, T., Kupiainen-Määttä, O., Loukonen, V., Kurtén, T., & Vehkamäki, H. (2014). Electrical charging changes the composition of sulfuric acid-ammonia/dimethylamine clusters. *Atmospheric Chemistry and Physics*, *14*(15), 7995–8007. https://doi.org/10.5194/acp-14-7995-2014

Passananti, M., Zapadinsky, E., Zanca, T., Kangasluoma, J., Myllys, N., Rissanen, M. P., Kurtén, T., Ehn, M., Attoui, M., & Vehkamäki, H. (2019). How well can we predict cluster fragmentation inside a mass spectrometer? *Chemical Communications*, *55*(42), 5946–5949. https://doi.org/10.1039/c9cc02896j

Peräkylä, O. (2020). *Production of condensible vapours from monoterpene oxidation* (Thesis). University of Helsinki. http://urn.fi/URN:ISBN:978-952-7276-38-9

Peräkylä, O., Riva, M., Heikkinen, L., Quéléver, L., Roldin, P., & Ehn, M. (2020). Experimental investigation into the volatilities of highly oxygenated organic molecules (HOMs). *Atmospheric Chemistry and Physics*, *20*(2), 649–669. https://doi.org/10.5194/acp-20-649-2020

Petäjä, T., Mauldin III, R. L., Kosciuch, E., McGrath, J., Nieminen, T., Paasonen, P., Boy, M., Adamov, A., Kotiaho, T., & Kulmala, M. (2009). Sulfuric acid and OH concentrations in a boreal forest site. *Atmospheric Chemistry and Physics*, *9*(19), 7435–7448. https://doi.org/10.5194/acp-9-7435-2009

Petäjä, T., Sipilä, M., Paasonen, P., Nieminen, T., Kurtén, T., Ortega, I. K., Stratmann, F., Vehkamäki, H., Berndt, T., & Kulmala, M. (2011). Experimental observation of strongly bound dimers of sulfuric acid: Application to nucleation in the atmosphere. *Physical Review Letters*, *106*(22). https://doi.org/10.1103/physrevlett.106.228302

Prisle, N. L., Raatikainen, T., Laaksonen, A., & Bilde, M. (2010). Surfactants in cloud droplet activation: Mixed organic-inorganic particles. *Atmospheric Chemistry and Physics*, *10*(12), 5663–5683. https://doi.org/10.5194/acp-10-5663-2010

Riccobono, F., Schobesberger, S., Scott, C. E., Dommen, J., Ortega, I. K., Rondo, L., Almeida, J., Amorim, A., Bianchi, F., ... Baltensperger, U. (2014). Oxidation products of biogenic emissions contribute to nucleation of atmospheric particles. *Science*, *344*(6185), 717–721. https://doi.org/10.1126/science.1243527

Richters, S., Herrmann, H., & Berndt, T. (2016a). Different pathways of the formation of highly oxidized multifunctional organic compounds (HOMs) from the gas-phase ozonolysis of β-caryophyllene. *Atmospheric Chemistry and Physics*, *16*(15), 9831–9845. https://doi.org/10.5194/acp-16-9831-2016

Richters, S., Herrmann, H., & Berndt, T. (2015). Gas-phase rate coefficients of the reaction of ozone with four sesquiterpenes at 295 $\pm$ 2 K. *Physical Chemistry Chemical Physics*, *17*(17), 11658–11669. https://doi.org/10.1039/c4cp05542j

Richters, S., Herrmann, H., & Berndt, T. (2016b). Highly oxidized RO_2 radicals and consecutive products from the ozonolysis of three sesquiterpenes. *Environmental Science & Technology*, *50*(5), 2354–2362. https://doi.org/10.1021/acs.est.5b05321

Riipinen, I., Pierce, J. R., Yli-Juuti, T., Nieminen, T., Häkkinen, S., Ehn, M., Junninen, H., Lehtipalo, K., Petäjä, T., ... Kulmala, M. (2011). Organic condensation: A vital link connecting aerosol formation to cloud condensation nuclei (CCN) concentrations. *Atmospheric Chemistry and Physics*, *11*(8), 3865–3878. https://doi.org/10.5194/acp-11-3865-2011

Riipinen, I., Yli-Juuti, T., Pierce, J. R., Petäjä, T., Worsnop, D. R., Kulmala, M., & Donahue, N. M. (2012). The contribution of organics to atmospheric nanoparticle growth. *Nature Geoscience*, *5*(7), 453–458. https://doi.org/10.1038/ngeo1499

Rinne, J., Back, J., & Hakola, H. (2009). Biogenic volatile organic compound emissions from the Eurasian taiga: current knowledge and future directions. *Boreal Environment Research*, *14*(4), 807–826.

Rissanen, M. P. (2018). NO_2 suppression of autoxidation–inhibition of gas-phase highly oxidized dimer product formation. *ACS Earth and Space Chemistry*, *2*(11), 1211–1219. https://doi.org/10.1021/acsearthspacechem.8b00123

Rissanen, M. P., Kurtén, T., Sipilä, M., Thornton, J. A., Kangasluoma, J., Sarnela, N., Junninen, H., Jørgensen, S., Schallhart, S., ... Ehn, M. (2014). The formation of highly oxidized multifunctional products in the ozonolysis of cyclohexene. *Journal of the American Chemical Society*, *136*(44), 15596–15606. https://doi.org/10.1021/ja507146s

Rissanen, M. P., Kurtén, T., Sipilä, M., Thornton, J. A., Kausiala, O., Garmash, O., Kjaergaard, H. G., Petäjä, T., Worsnop, D. R., ... Kulmala, M. (2015). Effects of chemical complexity on the autoxidation mechanisms of endocyclic alkene ozonolysis products: From methylcyclohexenes toward understanding α-pinene. *The Journal of Physical Chemistry A*, *119*(19), 4633–4650. https://doi.org/10.1021/jp510966g

Riva, M., Rantala, P., Krechmer, J. E., Peräkylä, O., Zhang, Y., Heikkinen, L., Garmash, O., Yan, C., Kulmala, M., ... Ehn, M. (2019). Evaluating the performance of five different chemical ionization techniques for detecting gaseous oxygenated organic species. *Atmospheric Measurement Techniques*, *12*(4), 2403–2421. https://doi.org/10.5194/amt-12-2403-2019

Rondo, L., Ehrhart, S., Kürten, A., Adamov, A., Bianchi, F., Breitenlechner, M., Duplissy, J., Franchin, A., Dommen, J., ... Curtius, J. (2016). Effect of dimethylamine on the gas phase sulfuric acid concentration measured by chemical ionization

mass spectrometry. *Journal of Geophysical Research: Atmospheres*, *121*(6), 3036–3049. https://doi.org/10.1002/2015jd023868

Rose, C., Zha, Q., Dada, L., Yan, C., Lehtipalo, K., Junninen, H., Mazon, S. B., Jokinen, T., Sarnela, N., ... Kulmala, M. (2018). Observations of biogenic ion-induced cluster formation in the atmosphere. *Science Advances*, *4*(4), eaar5218. https://doi.org/10.1126/sciadv.aar5218

Sarnela, N., Jokinen, T., Nieminen, T., Lehtipalo, K., Junninen, H., Kangasluoma, J., Hakala, J., Taipale, R., Schobesberger, S., ... Kulmala, M. (2015). Sulphuric acid and aerosol particle production in the vicinity of an oil refinery. *Atmospheric Environment*, *119*, 156–166. https://doi.org/10.1016/j.atmosenv.2015.08.033

Schobesberger, S., Franchin, A., Bianchi, F., Rondo, L., Duplissy, J., Kürten, A., Ortega, I. K., Metzger, A., Schnitzhofer, R., ... Worsnop, D. R. (2015). On the composition of ammonia–sulfuric-acid ion clusters during aerosol particle formation. *Atmospheric Chemistry and Physics*, *15*(1), 55–78. https://doi.org/10.5194/acp-15-55-2015

Schobesberger, S., Junninen, H., Bianchi, F., Lonn, G., Ehn, M., Lehtipalo, K., Dommen, J., Ehrhart, S., Ortega, I. K., ... Worsnop, D. R. (2013). Molecular understanding of atmospheric particle formation from sulfuric acid and large oxidized organic molecules. *Proceedings of the National Academy of Sciences*, *110*(43), 17223–17228. https://doi.org/10.1073/pnas.1306973110

Schwantes, R. H., Schilling, K. A., McVay, R. C., Lignell, H., Coggon, M. M., Zhang, X., Wennberg, P. O., & Seinfeld, J. H. (2017). Formation of highly oxygenated low-volatility products from cresol oxidation. *Atmospheric Chemistry and Physics*, *17*(5), 3453–3474. https://doi.org/10.5194/acp-17-3453-2017

Seinfeld, J. H., & Pandis, S. N. (2016). *Atmospheric chemistry and physics: From air pollution to climate change*. Hoboken, New Jersey, John Wiley & Sons.

Shu, Y., & Atkinson, R. (1995). Atmospheric lifetimes and fates of a series of sesquiterpenes. *Journal of Geophysical Research*, *100*(D4), 7275–7281. https://doi.org/10.1029/95jd00368

Sihto, S.-L., Kulmala, M., Kerminen, V.-M., Maso, M. D., Petäjä, T., Riipinen, I., Korhonen, H., Arnold, F., Janson, R., ... Lehtinen, K. E. J. (2006). Atmospheric sulphuric acid and aerosol formation: Implications from atmospheric measurements

for nucleation and early growth mechanisms. *Atmospheric Chemistry and Physics*, *6*(12), 4079–4091. https://doi.org/10.5194/acp-6-4079-2006

Sindelarova, K., Granier, C., Bouarar, I., Guenther, A., Tilmes, S., Stavrakou, T., Müller, J.-F., Kuhn, U., Stefani, P., & Knorr, W. (2014). Global data set of biogenic voc emissions calculated by the megan model over the last 30 years. *Atmospheric Chemistry and Physics*, *14*(17), 9317–9341. https://doi.org/10.5194/acp-14-9317-2014

Sipilä, M., Sarnela, N., Jokinen, T., Junninen, H., Hakala, J., Rissanen, M. P., Petäjä, T., & Worsnop, D. R. (2015). Bisulphate-cluster based atmospheric pressure chemical ionization mass spectrometer for ultra-high sensitivity (10 ppq) detection of atmospheric amines: Proof-of-concept and first ambient data from boreal forest. *Atmospheric Measurement Techniques Discussions*, *8*(4), 3667–3696. https://doi.org/10.5194/amtd-8-3667-2015

Sipilä, M., Sarnela, N., Jokinen, T., Henschel, H., Junninen, H., Kontkanen, J., Richters, S., Kangasluoma, J., Franchin, A., ... O'Dowd, C. (2016). Molecular-scale evidence of aerosol particle formation via sequential addition of HIO_3. *Nature*, *537*(7621), 532–534. https://doi.org/10.1038/nature19314

Taggart, R. E., & Cross, A. T. (2009). Global greenhouse to icehouse and back again: The origin and future of the boreal forest biome. *Global and Planetary Change*, *65*(3-4), 115–121. https://doi.org/10.1016/j.gloplacha.2008.10.014

Tarvainen, V., Hakola, H., Rinne, J., Hellén, H., & Haapanala, S. (2007). Towards a comprehensive emission inventory of terpenoids from boreal ecosystems. *Tellus B*, *59*(3), 526–534. https://doi.org/10.1111/j.1600-0889.2007.00263.x

Thomson, W. (1871). LX. on the equilibrium of vapour at a curved surface of liquid. *The London, Edinburgh, and Dublin Philosophical Magazine and Journal of Science*, *42*(282), 448–452. https://doi.org/10.1080/14786447108640606

Thornton, J. A., Kercher, J. P., Riedel, T. P., Wagner, N. L., Cozic, J., Holloway, J. S., Dubé, W. P., Wolfe, G. M., Quinn, P. K., ... Brown, S. S. (2010). A large atomic chlorine source inferred from mid-continental reactive nitrogen chemistry. *Nature*, *464*(7286), 271–274. https://doi.org/10.1038/nature08905

Tröstl, J., Chuang, W. K., Gordon, H., Heinritzi, M., Yan, C., Molteni, U., Ahlm, L., Frege, C., Bianchi, F., ... Baltensperger, U. (2016). The role of low-volatility organic

compounds in initial particle growth in the atmosphere. *Nature*, *533*(7604), 527–531. https://doi.org/10.1038/nature18271

Tsiligiannis, E., Hammes, J., Salvador, C. M., Mentel, T. F., & Hallquist, M. (2019). Effect of NO_x on 1,3,5-trimethylbenzene (TMB) oxidation product distribution and particle formation. *Atmospheric Chemistry and Physics*, *19*(23), 15073–15086. https://doi.org/10.5194/acp-19-15073-2019

Twomey, S. (1977). The Influence of Pollution on the Shortwave Albedo of Clouds. *Journal of the Atmospheric Sciences*, *34*(7), 1149–1152. https://doi.org/10.1175/1520-0469(1977)034⟨1149:TIOPOT⟩2.0.CO;2

Twomey, S. (1991). Aerosols, clouds and radiation. *Atmospheric Environment. Part A. General Topics*, *25*(11), 2435–2442. https://doi.org/10.1016/0960-1686(91)90159-5

Tyndall, J. (1869). IV. on the blue colour of the sky, the polarization of skylight, and on the polarization of light by cloudy matter generally. *Proceedings of the Royal Society of London*, *17*, 223–233. https://doi.org/10.1098/rspl.1868.0033

Vanhanen, J., Mikkilä, J., Lehtipalo, K., Sipilä, M., Manninen, H. E., Siivola, E., Petäjä, T., & Kulmala, M. (2011). Particle size magnifier for nano-cn detection. *Aerosol Science and Technology*, *45*(4), 533–542. https://doi.org/10.1080/02786826.2010.547889

Vehkamäki, H. (2006). *Classical nucleation theory in multicomponent systems*. Springer, Berlin, Heidelberg.

Vehkamäki, H., & Riipinen, I. (2012). Thermodynamics and kinetics of atmospheric aerosol particle formation and growth. *Chemical Society Reviews*, *41*(15), 5160. https://doi.org/10.1039/c2cs00002d

Vereecken, L., & Francisco, J. S. (2012). Theoretical studies of atmospheric reaction mechanisms in the troposphere. *Chemical Society Reviews*, *41*(19), 6259. https://doi.org/10.1039/c2cs35070j

Volkamer, R., Martini, F. S., Molina, L. T., Salcedo, D., Jimenez, J. L., & Molina, M. J. (2007). A missing sink for gas-phase glyoxal in Mexico City: Formation of secondary organic aerosol. *Geophysical Research Letters*, *34*(19). https://doi.org/10.1029/2007gl030752

Wang, S., Wu, R., Berndt, T., Ehn, M., & Wang, L. (2017). Formation of highly oxidized radicals and multifunctional products from the atmospheric oxidation of

alkylbenzenes. *Environmental Science & Technology*, *51*(15), 8442–8449. https://doi.org/10.1021/acs.est.7b02374

Wang, Y., Mehra, A., Krechmer, J. E., Yang, G., Hu, X., Lu, Y., Lambe, A., Canagaratna, M., Chen, J., ... Wang, L. (2020). Oxygenated products formed from oh-initiated reactions of trimethylbenzene: Autoxidation and accretion. *Atmospheric Chemistry and Physics*, *20*(15), 9563–9579. https://doi.org/10.5194/acp-20-9563-2020

Weber, R. J., Marti, J. J., McMurry, P. H., Eisele, F. L., Tanner, D. J., & Jefferson, A. (1996). Measured atmospheric new particle formation rates: Implications for nucleation mechanisms. *Chemical Engineering Communications*, *151*(1), 53–64. https://doi.org/10.1080/00986449608936541

Went, F. W. (1960). Blue hazes in the atmosphere. *Nature*, *187*(4738), 641–643. https://doi.org/10.1038/187641a0

Wildt, J., Mentel, T. F., Kiendler-Scharr, A., Hoffmann, T., Andres, S., Ehn, M., Kleist, E., Müsgen, P., Rohrer, F., ... Wahner, A. (2014). Suppression of new particle formation from monoterpene oxidation by NO_x. *Atmospheric Chemistry and Physics*, *14*(6), 2789–2804. https://doi.org/10.5194/acp-14-2789-2014

Yan, C., Nie, W., Vogel, A. L., Dada, L., Lehtipalo, K., Stolzenburg, D., Wagner, R., Rissanen, M. P., Xiao, M., ... Worsnop, D. R. (2020). Size-dependent influence of NO_x on the growth rates of organic aerosol particles. *Science Advances*, *6*(22), eaay4945. https://doi.org/10.1126/sciadv.aay4945

Yan, C., Nie, W., Äijälä, M., Rissanen, M. P., Canagaratna, M. R., Massoli, P., Junninen, H., Jokinen, T., Sarnela, N., ... Ehn, M. (2016). Source characterization of highly oxidized multifunctional compounds in a boreal forest environment using positive matrix factorization. *Atmospheric Chemistry and Physics*, *16*(19), 12715–12731. https://doi.org/10.5194/acp-16-12715-2016

Yli-Juuti, T., Mohr, C., & Riipinen, I. (2020). Open questions on atmospheric nanoparticle growth. *Communications Chemistry*, *3*(1). https://doi.org/10.1038/s42004-020-00339-4

Zaytsev, A., Koss, A. R., Breitenlechner, M., Krechmer, J. E., Nihill, K. J., Lim, C. Y., Rowe, J. C., Cox, J. L., Moss, J., ... Keutsch, F. N. (2019). Mechanistic study of the formation of ring-retaining and ring-opening products from the oxidation of

aromatic compounds under urban atmospheric conditions. *Atmospheric Chemistry and Physics*, *19*(23), 15117–15129. https://doi.org/10.5194/acp-19-15117-2019

Zhang, R., Khalizov, A., Wang, L., Hu, M., & Xu, W. (2011). Nucleation and growth of nanoparticles in the atmosphere. *Chemical Reviews*, *112*(3), 1957–2011. https://doi.org/10.1021/cr2001756

Zhang, Y., Peräkylä, O., Yan, C., Heikkinen, L., Äijälä, M., Daellenbach, K. R., Zha, Q., Riva, M., Garmash, O., ... Ehn, M. (2020). Insights into atmospheric oxidation processes by performing factor analyses on subranges of mass spectra. *Atmospheric Chemistry and Physics*, *20*(10), 5945–5961. https://doi.org/10.5194/acp-20-5945-2020